RSC Advances

REVIEW

View Article Online
View Journal | View Issue

Cite this: *RSC Adv.*, 2024, **14**, 12984

Smart materials for flexible electronics and devices: hydrogel

Taposhree Dutta,[a] Pavan Chaturvedi,[b] Ignacio Llamas-Garro,[c] Jesús Salvador Velázquez-González,[c] Rakesh Dubey[d] and Satyendra Kumar Mishra*[e]

Received 15th February 2024
Accepted 5th April 2024

DOI: 10.1039/d4ra01168f

rsc.li/rsc-advances

In recent years, flexible conductive materials have attracted considerable attention for their potential use in flexible energy storage devices, touch panels, sensors, memristors, and other applications. The outstanding flexibility, electricity, and tunable mechanical properties of hydrogels make them ideal conductive materials for flexible electronic devices. Various synthetic strategies have been developed to produce conductive and environmentally friendly hydrogels for high-performance flexible electronics. In this review, we discuss the state-of-the-art applications of hydrogels in flexible electronics, such as energy storage, touch panels, memristor devices, and sensors like temperature, gas, humidity, chemical, strain, and textile sensors, and the latest synthesis methods of hydrogels. Describe the process of fabricating sensors as well. Finally, we discussed the challenges and future research avenues for flexible and portable electronic devices based on hydrogels.

1. Introduction

Flexible electronics comprise circuits and components that can be bent, rolled, folded and stretched without losing their ability to work. In 1960s, tiny, flexible solar cells were developed for satellites, which rise the idea of flexible electronics.[1] Advanced, flexible, and large-processable materials have since been developed, including conductive polymers, organic semiconductors, and amorphous silicon. Integrated electronic components directly onto flexible substrates have gained popularity in recent years.[2–4] In recent years, flexible electronics have gained increasing amounts of applications, such as flexible sensors, energy harvesters, batteries, transformers, display screens, *etc.*[5,6] Unlike traditional, rigid, and brittle electronics, future electronics must be lighter, more portable, biocompatible, wearable, and provide better mechanical stability.[7–9] A flexible electronics device is made from inorganic or organic compounds, such as metal nanoparticles or nanowires, metal oxides, carbon, or polymers coated with conductive materials. Due to development of flexible electronics, which interface living biological tissues with synthetic electronic systems—also known as bioelectronics or bio-integrated wearable systems.[10]

It has been widely recognized that flexible electronics can be used as multipurpose interfaces between hard surfaces of traditional medical monitoring devices and soft tissues within the human body.[11–13] As a vital indicator of health, the human body continuously fluctuates for various biological signals. The signals include body temperature, blood pressure, glucose, and perspiration, as well as an electroencephalogram, an electrocardiogram, and an electroencephalogram. Biosensors, particularly flexible electronics, have proven promising as a way to gather medical diagnostic information directly and efficiently. The biocompatible, mechanically flexible, and durable nature of flexible electronics makes them easy to integrate into soft tissues and organs. To provide a variety of capabilities, they are also combined with electronic components. Due to the rapid development of biosensors, wearable and portable electronics are becoming increasingly important. A few other fields where flexible electronics with stimuli-responsive properties can find practical application include energy harvesting devices, biosensors, smart actuators, artificial muscles, and skins, drug delivery systems, wearable displays, and touch panels.

In conventional flexible electronics designs, active devices are usually positioned on islands, organic base materials are insulated, and conductive interconnects are carefully crafted. Researchers have made significant advances in flexible electronics fabrication since the first "Sensitive Skin Workshop" in 1999.[14] Inverted configurations combining interconnect metal, gate metal, source/drain metal, and dielectrics were used to deposit organic semiconductor transistor circuits directly on

[a]*Department of Chemistry, Indian Institute of Engineering Science and Technology Shibpur, Howrah, W.B. – 711103, India*
[b]*Department of Physics, Vanderbilt University, 3414 Murphy Rd, Apt#4, Nashville, TN-37203, USA*
[c]*Navigation and Positioning Research Unit, Centre Tecnològic de Telecomunicacions de Catalunya Castelldefels, Spain*
[d]*Instiute of Physics, University of Szczecin, Poland*
[e]*Space and Reslinent Research Unit, Centre Tecnològic de Telecomunicacions de Catalunya Castelldefels, Spain. E-mail: smishra@cttc.es*

flexible printed wiring boards. Transistors could be integrated on a large scale and for a long time as a result of this. Applying gold nanofilm stripes on pre-stretched dielectric elastomeric membranes of polydimethylsiloxane (PDMS), Suo *et al.* created spontaneously wrinkled metal strips that served as stretchy electrical interconnects for flexible electronics circuits.[15] Using a sacrificial poly(methyl methacrylate) layer as a temporary support for the build-up of ICs on a thin polyimide or PDMS layer and sandwiching them between another thin layer of polyimide or PDMS, Rogers *et al.* Designed a novel configuration of silicon complementary metal-oxide semiconductor integrated circuits (ICs) to withstand extreme mechanical conditions, such as large deformations and foldability.[16] Due to their low critical strain, metal film stripes have been replaced by elastic conductors such as polymer composites and single-walled carbon nanotubes (CNTs) for improved stretchability.[17] Bao *et al.* developed flexible organic field-effect transistor devices based on micro structured dielectric elastomer PDMS sheets to mimic the sensing characteristics of natural skin. By adjusting the capacitance in response to pressure, these devices could easily be used.[18] A multilayer arrangement remains one of the simplest and most advanced approaches to fabricating flexible electronics to date. Polymeric elastomers can act as effective carrier matrixes for integrating conducting materials. The assembly of surfaces with mechanical mismatches, particularly stretchability, usually results in interface delamination and flaws. Several elastomers are also incompatible with human tissues biologically and mechanically.[11,19,20] As part of the development of flexible electronics, particularly in the field of biosensors, conductive hydrogels (CHs) have attracted significant interest in the last twenty years. This is due to their exceptional biocompatibility, tuneable mechanical flexibility, good conductivity, and multi-stimulation responsive properties.[21]

Hydrogels were porous polymer networks with a high-water content that showed great promise for various uses, such as tissue engineering, controlled drug administration, actuators, and sensors. Soft robotics, electronic skins, energy conversion, and health diagnosis are a few of the new fields that benefit from hydrogels' ability to combine conductivity and mechanical properties. Conductivity is a result of both ion and electron transport. Humans and animals use ions to transmit electrical information, while inorganic materials like metals use electrons to conduct electricity. Conductive hydrogels are thus designed by adding ions or electrons to the hydrogel matrix. It is common for electron-conductive hydrogels to be used in bioengineering applications such as drug delivery systems, tissue engineering systems, and biosensors because they are compatible with biological tissues as opposed to ion–ion-conductive hydrogels, which leak and diffuse ions into the surrounding environment. In energy storage and conversion devices such as actuators and nanogenerators, as well as touch screens and displays, ion–CHs are highly desirable because they have ion gradients and are transparent.

Since hydrogel mimics the mechanical, chemical, and optical properties of biological tissues, it has great potential as a flexible electronics material. Due to their elevated water content, hydrophilic crosslinked polymer hydrogels exhibit dual-phase behavior.[22] Hydrogel coatings, hydrogel optics, and other potential applications as machines have been studied by Zhao *et al.*[22,23] Guo *et al.* investigated the structure, characteristics, and uses of stimuli-responsive conductive hydrogels.[24] The next generation of materials for making supercapacitors is known as functional hydrogels. As a result of their unique properties and flexibility, hydrogels are suitable for wearable applications.[25] Ionic-based hydrogels are used for energy storage in this regard. As a result of their ease of processing, sustainability, and environmental friendliness, hydrogels are considered the next generation of materials.

A flexible electronic device can benefit from hydrogel's specific properties, such as its straightforward processing, conductivity, tuneable mechanical flexibility, and good electrical properties. Recent years have seen an increase in research into conductive hydrogels. The emergence of flexible electronics has opened up new possibilities for electrodes, mechanical sensors, displays, and other devices that involve the human body.[26–28] To realize flexible electronics based on hydrogels, it is imperative to develop conductive hydrogel materials with good carrier mobility and electrical performance.[29,30] In this article, we provide a brief overview of development of different conductive hydrogels and focus on their various applications in flexible electronics and devices, such as sensors, energy storage devices, and touch screens (Fig. 1). In addition, techniques to enhance hydrogel activity were discussed. A future perspective for multifunctional hydrogel-based flexible electronics and devices is also presented.

2. Hydrogels

An hydrogel is a network of three-dimensional polymers that can store and hold large amounts of fluid within their own structure, this phenomenon is known as swelling. This swelling behaviour is caused by a physical or chemical crosslinking of

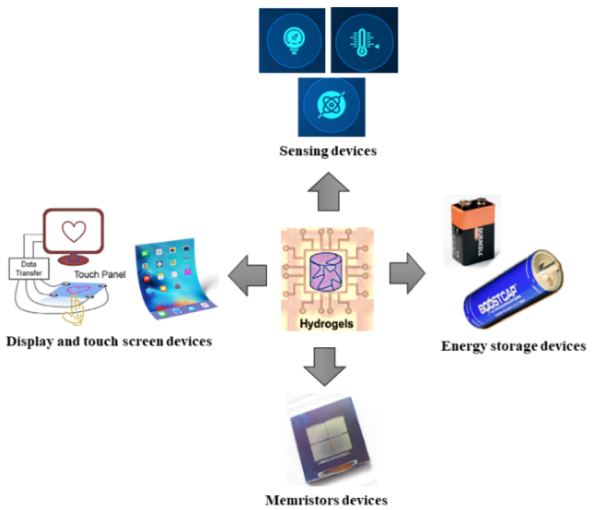

Fig. 1 Schematic view of hydrogels used in various applications in flexible electronics and devices.

the polymer chains that maintain the network structure. Hydrogels made from natural materials, like plants and animals, are known as natural hydrogels. Natural polymers include cellulose, alginate, chitosan, and gelatin.[31] It is possible to produce hydrogels using synthetic, natural, or a combination of both sources. Tang *et al.* developed synthetic hydrogel using chitosan.[32] Synthetic hydrogels made from synthetic polymers created by chemical polymerization techniques, such as polyethylene glycol (PEG), polylactic acid, polycaprolactone (PCL), and polyvinyl alcohol (PVA).

3. Types of hydrogels used for flexible electronics and devices

Several cutting-edge fields have been advanced by hydrogels by combining mechanical properties and conductivity, including energy conversion, electronic skin, soft robotics, and health diagnosis.[32] The transport of electrons or ions determines the conductivity in nature. Living things such as humans and animals carry electrical information with ions, while materials conduct current with electrons. In Table 1, the mechanisms, conductivities, and optical properties of conductive materials are summarized. A few types of hydrogels based on conductivity properties are discussed below.

3.1 Electron-conductive hydrogels

Hydrogels based on electron conductivity were used in flexible electronics and devices.[33,34] Generally, electron-conducting materials divide into three classes: (i) metallic nanoparticles, such as Au, Ag, and Cu nanoparticles, *etc.*; (ii) carbon-based nanomaterials, such as carbon nanoparticles, carbon nanowires, carbon nanosheets, graphene, graphene oxide (GO), reduced GO (rGO) nanosheets, *etc.*, (iii) polymers, such as polyaniline, polypyrene, poly(phenylene vinylene), polythiophene, and [PEDOT:PSS], and (iv) hybrid conducting based electron conductive hydrogels.

3.1.1 Metal nanoparticles-based electron-conductive hydrogels. A metallic nanomaterial is used extensively to synthesize metal nanoparticles-based conductive hydrogels (Fig. 2(a)), due to its unique properties, including high electrical conductivity, high specific surface energy, optical, magnetic, and catalytic properties.[35] Among pure metals, silver exhibits the greatest electrical conductivity, and Ag nanomaterials exhibit outstanding electron transport abilities. Several researchers have exploited these properties to prepare highly conductive hydrogels.

According to Xiang *et al.*, deproteinized carboxylic acid groups are bonded to Ag^+ hydrogel networks so that they do not clump together. Following this, Ag^+ ions were reduced into Ag nanoparticles *via* CH, which were pH-responsive electrically.[36] A homogeneous network of electron-conductive hydrogels was developed by Devaki *et al.* through the combination of *in situ* Ag^+ reduction and acrylic acid polymerization.[37] Zhao *et al.* developed thermo-switchable electron-conductive hydrogels by copolymerizing vinyl-functionalized Au nanoparticles with NIPAM.[38] Using "breathing" mechanism, Willner *et al.*

Table 1 Various types of conductive hydrogels

Types of conductive hydrogels	Conductive components	Materials	Conductivity (S m^{-1})	Application	References
Electron-conductive hydrogels	Metallic nanoparticles	Ag/Au/Cu nanoparticles	0.057–2.2 × 10^7	Biosensor, tissue engineering, drug delivery	37 and 48–53
	Carbon based materials	CNT/graphene/GO/rGO	0.072–8.2; 1.56 × 10^{-5}	Strain sensor, supercapacitor	39 and 54–60
	Conducting polymers	Polyanilline, PEDOT:PSS	1 × 10^{-3}–43; 1.5 × 10^{-3}–4000	Biosensor, strain sensor	41 and 61–71
	Hybrid	Pt/Ag/GO + rGO/SWCNT + polyaniline	13.64–21	Battery, fuel cell, strain sensor	42,72,73
Ion-conductive hydrogels	Acids, metallic salts	H_2SO_4/H_3PO_4, LiCl/Na^+/Ca^{2+}/Al^3/Fe^{3+}/Tb^{3+}/K^+	8.2, 1.25 × 10^{-3}	Solar cell, nanogenerator	45 and 74–89
Electro-ion-conductive hydrogels	Electron-conductive components and ions	Na^+ + Au nanoparticles, Fe^{3+} + polypyrrole/rGO	0.45–2.92, 880	Strain sensor, biosensor, supercapacitor	90–92

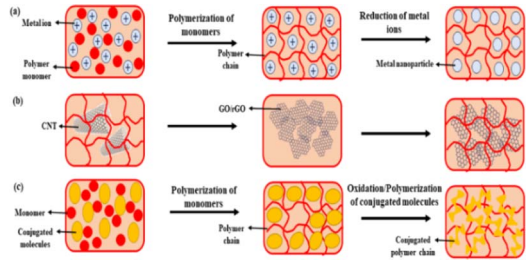

Fig. 2 Schematic illustration of fabrication process of (a) metal nano particle doped electron-conductive hydrogels; (b) carbon material-based electron-conductive hydrogels; (c) conjugated polymer-based electron-conductive hydrogels.

synthesized Au-loaded hydrogels, in which the polyacrylamide (PAM) hydrogels swell in aqueous solution containing Au nanoparticles and shrink in acetone immobilized nanoparticles in polymer network.[38] By reducing Cu^{2+} within a PVA network grafted with PAM branches, Cu nanoparticles were created *in situ*, resulting in conductive hydrogels for vapor detection.[38]

3.1.2 Carbon material-based electron-conductive hydrogels. The use of carbon-based materials, such as graphene and carbon nanotubes (CNTs), is a promising approach for creating three-dimensional electron-conductive networks within polymer matrixes (Fig. 2(b)). Besides creating pathways for electron transport, these networks also improve the mechanical properties of the materials thanks to their large surface area and numerous surface functionalities.[38] As shown in Fig. 2(b), conductive hydrogels such as CNT/GO/rGO based hydrogels can be constructed using conductive elements in hydrogel matrixes or through cross-linking GO nanosheets to build 3D networks. Using acrylic acid and acrylamide solutions, adhesive conductive hydrogels were synthesized on nanotubes decorated with polydopamine. As long-lasting strain sensors in harsh environments, these CNTs have demonstrated anti-freezing and anti-heating properties. CNTs and LAPONITE® nano-clays were doped into poly(*N*-isopropyl acrylamide) hydrogels to produce thermally and photothermally responsive conductive hydrogels with high stretchability, self-healing, adhesiveness, and 3D printability. By heating GO and hydroquinone aqueous solution, Xu *et al.* described a functionalized graphene hydrogel which could be used as a supercapacitor electrode. Additionally, hydroquinone inside graphene frameworks functioned as a pseudocapacitive element, helping to reduce GO to graphene.[39]

3.1.3 Polymer-based electron-conductive hydrogels. In compared to other conducting materials, conducting polymers have recently gained attention for manufacturing conductive hydrogels because of their many benefits, including adjustable electronic conductivity, biocompatibility, flexibility, and versatile solubility when reduced.[40] PEDOT:PSS, polyaniline, and polypyrrole were the most commonly used conducting polymers. A conducting polymer had a unique π-conjugated structure for electron transport. Fig. 2(c) showed schematic images of typical designs of conducting polymer-based electron-conductive hydrogels. A poly(2-acrylamido-2-methyl-1-propane sulfonic acid)/poly(ethylene glycol) diglyceryl ether cross-linked electrostatic adduct of emeraldine-polyaniline can be prepared by *in situ* polymerizing aniline in aqueous poly(2-acrylamido-2-methyl-1-propane sulfonic acid) solution. This led to the development of redox conductive hydrogels for glucose electrooxidation catalysis. Li *et al.* designed hydrogel electrodes for high-performance flexible supercapacitors by combining boronate-bearing polyaniline with PVA.[38] A freeze–thaw process controls the microstructure and mechanical properties of conductive hydrogels. Han *et al.* developed a transparent polypyrrole-containing conductive hydrogel by *in situ* converting polydopamine–polypyrrole nanoparticles in PAM matrix into polydopamine–polypyrrole nanofibrils.[38] In a study by Gavottes *et al.*, PVA was incorporated with PEDOT:PSS as conductive components, and ethylene glycol and iota-carrageenan were used to reinforce the intermolecular interactions.[41]

3.1.4 Hybrid conducting materials based electron-conductive hydrogels. In order to achieve desired electrical and mechanical properties, many electron-conductive hydrogels are combined with various conducting materials. Metallic nanoparticles and polymers containing conducting polymers are among the common types of conductive hydrogels. In a study published in Nature Chemical Biology, Yu *et al.* fabricated a homogenous high-density polyaniline hydrogel loaded with Pt nanoparticles that were used for sensitive glucose sensors and metabolites (such as uric acid and cholesterol) detection devices.[42] The presence of single-walled CNTs (SWCNTs) in PVA–H_2SO_4 hydrogel could induce the polymerization of anilines, resultant all-in-one configured flexible supercapacitor with a better capacitive performance of 15.8 mF cm^{-2} at 0.044 mA cm^{-2} current density, compared with pure SWCNTs (0.16 mF cm^{-2}) or poly-aniline (3.85 mF cm^{-2}).[43] To improving the specific capacitance, cyclic stability, and energy density of CuS or GO supercapacitors, hydrothermal reaction of GO conductive hydrogels decorated with carbon dots-supported copper sulphide was employed as the positive electrode of an asymmetric supercapacitor, where rGO served as the negative electrode.[38]

3.2 Ion-conductive hydrogels

There was a network of polymers in hydrogels that contained a great deal of water, as well as a porous structure that allowed water molecules to freely flow between the polymer networks. Due to the high mobility of water-soluble ions, it is possible to design ion-conductive hydrogel-based flexible electronics and devices. There are three types of materials that produce free ions in water: (i) acids, such as H_2SO_4, HCl, H_3PO_4; metallic salts, such as NaCl/Na_2SO_4, KCl, LiCl, $LiClO_4$, $FeCl_3$/$FeNO_3$, $CaCO_3$/$CaCl_2$, $TbCl_3$, $AlCl_3$, and ionic liquids, such as 1-ethyl-3-methylimidazolium chloride. Ion-conductive hydrogels had several advantages over electron-conductive hydrogels, and their special properties expand the possibilities for flexible electronics. Ion-conductive hydrogels are used as electrolytes in solid batteries and as actuators.[44]

3.3 Electron and ion-conductive hydrogels

Combining ion and electron-conductive materials in one hydrogel could achieve the advantages of both. Conducting

polymers, such as polyaniline, PEDOT:PSS, and H^+, can be used to develop CH electrodes with excellent performance. In many cases, HCl, $HClO_4$, and H_2SO_4 were combined synergistically. The flexible supercapacitor is combined with polyaniline hydrogel electrodes doped with $HClO_4$ and embedded in a PVA–H_2SO_4 hydrogel electrolyte.[45] Using interactions between Fe^{3+} and carboxy groups of gelatine chains and catechol groups of tethered dopamine molecules, a paintable adhesive conductive.

Hydrogel has been developed as a therapeutic cardiac patch. Tetra-sulfonic acid functional groups, copper phthalocyanine-3,4′,4″,4‴-tetra sulfonic acid tetrasodium salt (CuPcTs), a type of disc-shaped liquid crystal molecules, could form quadruple electrostatic interactions with positively charged polypyrrole chains; it produced an interconnected nanofiber structure that demonstrated higher conductivity (780 S m^{-1}) than pristine polypyrrole hydrogel (7 S m^{-1}).[46]

4. Techniques to enhance hydrogel performance

4.1 Modification in conductivity

It is important to understand the methods used to improve hydrogels' conductive properties in light of the growing interest, design, and development of wearable sensors. There are four types of techniques: adding conductive dopants; selectively using conductive materials; introducing free ions; and adding a new network. Dopant graphene has a high charge carrier density and mobility, and an electrical conductivity of up to 6×10^5 S m^{-1}.[47] Polyacrylamide hydrogels were given conductivity by adding exfoliated graphene to micro engineered frameworks. With a mere 0.32 vol% addition of graphene, the conductivity of the polyacrylamide hydrogel rose from 0.006 to 1.8 S m^{-1}. In addition, a linear relationship was observed between the specific conductivity and the amount of graphene added to the hydrogel. To control the conductivity of the hydrogel, the concentration of the dopant can be adjusted. A study conducted by Minev *et al.* found that the double network technique was highly effective and produced a multi-network hydrogel scaffold with excellent stretchability, tissue-like elastic modulus, and electrical conductivity of $\approx$26 S m^{-1}.[93] For better matrix integration, Lu *et al.* hybridized and doped polypyrrole with hydrophilic polydopamine to improve its hydrophilicity.[69] Hydrogels resulting from this process demonstrated good conductivity.

4.2 Mechanical assistance

Hydrogel's mechanical weakness was resolved through researchers' ability to vary crosslinking density and monomer choice to make it more flexible. Although hydrogels contain a high proportion of water and resemble extracellular matrices in many ways, the high-water content also causes them to have weak mechanical properties. Adding dopants to hydrogels is a common method of improving their mechanical properties. Adding calcium carbonate as a dopant, for instance, modified the mechanical properties of acetate chitosan hydrogels and increased their storage moduli by approximately 60.88 Pa. The anisotropic structure was prepared by freezing casting PVA, and then microphase separation was introduced by submerging the constructed structure in sodium citrate solution.[94] It was found that the hydrogels achieved ultimate stress, ultimate strain, and fracture energy of 23.5 $\pm$ 2.7 MPa, 2900 $\pm$ 450%, and 170 $\pm$ 8 kJ m^{-2}, respectively.

The mechanical properties of hydrogels can be evaluated by a variety of methods, including frequency-based testing using rheometry and dynamic mechanical analysis, as well as compression and tension tests, which can be conducted by using a probe to indent the material in a restricted or unconfined manner. When performing frequency-based sinusoidal tests, rheometers are usually used. By placing the sample on an instrument with a certain geometry, a variety of sweep measurements can be performed. Hydrogels can be examined for viscoelastic characteristics using a rheometer. Rheology is the study of the deformability and movement of matter under stress or strain. The term comes from the Greek words "rheo", which means flow, and "-ology", which means study.[95] Following Maxwell and Wilhelm Weber's descriptions of fluids and silk thread's non-ideal behaviours, scientists began to be concerned. Maxwell reported and mathematically proved the elastic properties of fluids. A less-than-ideal elastic property of silk thread was also discovered by Wilhelm Weber. In general, these substances are classified as non-Newtonian and viscoelastic. The viscosity of non-Newtonian materials is dependent on time and stress, but viscoelastic materials are resilient. Stress and strain variables play a significant role in rheology. The definition of shear stress is "the force per unit area that generates disorder in the materials between plates". "The ratio of deviation in material displacement (x) to material height (h), or more simply expressed as tan α", which is known as strain. When force is applied to the material, the internal force controls the movement's velocity. To determine the mechanical properties of hydrogels, small deformation rheology tests can be performed. When force is applied to a hydrogel, the material particles are moved around one another. Moreover, elastic materials change shape when force is applied, resulting in elastic strain, and then return to their original shape when the force is released. A force applied to viscous materials, however, results in irreversible strain. It is this input force that causes the flow of viscous materials. Instead of being entirely viscous or elastic, hydrogels exhibit a viscoelastic quality. Rheological studies were conducted within the linear viscoelastic region (LVR) of the materials under investigation. It ensures that hydrogels' mechanical properties are not affected by the magnitude of the applied stress or strain. When a gradual external force is applied to viscoelastic materials, very little deformation occurs. Due to the still-close-to-equilibrium molecular configuration of polymers, it occurs. Mechanical behaviour is only a reflection of molecular dynamics, even for equilibrium systems.

Eqn (1) can be used to express the concept of shear strain for controlled-strain rheometers, which defined sinusoidal function of time (t).

$$\gamma_{(t)} = \gamma_{0 \sin(\omega t)} \quad (1)$$

where, γ_0 = magnitude of applied strain; ω = angular frequency of oscillation, it measured in rad s^{-1}.Here, $\omega = 2\pi f$, where f = frequency.

Moreover, sinusoidal stress produced by sinusoidal strain, as demonstrated in eqn (2).

$$\tau_{(t)} = \tau_0(\sin \omega t + \delta) \quad (2)$$

where, τ_0 = stress amplitude; δ = phase difference in between two waves.

Eqn (3) can be used to express the concept of shear stress for controlled-strain rheometers, which defined sinusoidal function of time (t).

$$\tau_{(t)} = \tau_0(\sin \omega t) \quad (3)$$

Eqn (4) provides an illustration of association of sinusoidal stress and strain.

$$\gamma_{(t)} = \gamma_0(\sin \omega t + \delta) \quad (4)$$

Stress and strain are always in phase according to Hooke's law for materials that are entirely flexible. Therefore, the phase angle is 0 ($\delta = 0°$). Viscose materials, on the other hand, exhibit two distinct waves with phase angles of 90° and 90°, respectively. Viscoelastic materials, however, have a phase angle between 0° and 90°. The shear storage modulus (G'), loss modulus (G''), and loss factor (tan δ) of hydrogels are important characteristics in small-amplitude oscillatory analysis. The ratio of G'' to G' (G''/G') is the loss factor, tan δ. More viscous properties occur in materials when tan δ is more than 1 ($G'' > G'$). Tan $\delta < 1$ ($G' > G''$), indicated that a material has higher elastic solid properties.

The mechanical properties of viscoelastic materials are independent of strain up to a certain point. When strain rises above threshold, the storage modulus decreases, and a nonlinear behaviour is evident. The initial stage determined a material's LVR at 1 Hz frequency, was performing strain-dependent G' and G'' measurements. Solid material properties demonstrated by the G' frequency independent below the critical strain. On the other hand, the fluid-like substance is represented by frequency-dependent G'. The sol–gel behaviour of thermo-gelling chitosan-graft (PEG–PAF) was observed by Jeong *et al.* At 10 and 37 °C, the storage and loss moduli were measured in relation to frequency.[96] At 10 °C, G'' was found to be higher than G' (sol behaviour), whereas at 37 °C, G' was found to be higher than G'' (gel behaviour). But frequency had no effect on the storage modulus.

4.3 Self-healing

Hydrogels with the ability to heal themselves are desirable, particularly for wearable sensors, since they can maintain their mechanical strength and elasticity over time, along with their network integrity. Wang *et al.* created a stretchable, adhesive, and self-repairing conductive structure colour film for double-signal flexible electronic devices by introducing conductive carbon nanotube polydopamine into an elastic polyurethane reverse opal scaffold.[97] As a result, the resulting film had a stable tensile property and bright colour structure, and its interactive colour change during the tensile process made it suitable for real-time colour displays. By infusing hydrophobic polyacrylamide (HAPAM), graphene oxide (GO), and LAPONITE® clay into the gel matrix, Cui *et al.* developed an intriguing hydrogel with improved mechanical properties.[98]

5. Fabrication of sensors

Many industries and the automobile sector have noticed an increase in the need for sensors. Recent advancements in the field of Herem we discussed the fabrication of sensors. It primarily focused on advancements in techniques such as printing, etching, and deposition.

5.1 Deposition

"Deposition" refers to a wide range of processes, including chemical vapour deposition, sputtering, and the deposition of oxides, metals, and nonmetals. In microfabrication, atomic layer deposition (ALD) is a novel technique that has recently emerged and is considered a subclass of chemical vapour deposition. In ALD, gas-phase chemical reactions are systematically used to deposit thin films. Various compounds are used in the process to deposit thin films on the substrate gradually. Fig. 3 illustrates the thin layer deposition initiative *via* ALD. As a result of low-temperature deposition or ALD, atomic layers are better conformed and controllable in thickness and composition. A number of micro/nanodevices/features have been made, including nano CMOS, nanodot memory, non-volatile memory, TFTs, LEDs, nanolaminates, nanotubes, nanoalloys, *etc.*[99] ALD has also been used to fabricate micro/nano devices that are used as automobile sensors. ALD is used in the fabrication of various nanodevices, including 1D FETs, high mobility FETs, and non-volatile memory devices, which are used in electrical sensors and detectors. Moreover, Gong *et al.* have applied ZrO_2 films through ALD to the surface of a highly active but unstable solid oxide fuel cell cathode.[100] ALD was found to significantly reduce the area specific resistance and degradation rate of CNTs because of increasing oxygen reduction reaction activity.[97]

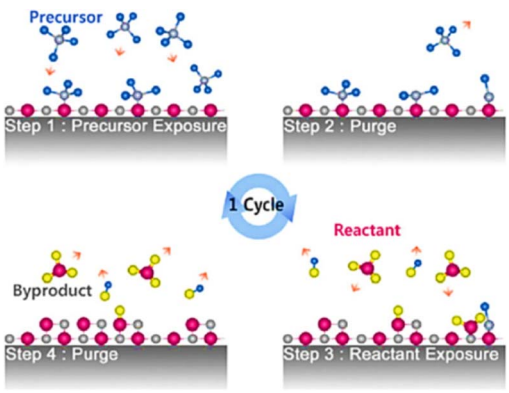

Fig. 3 Schematic diagram of thin layer formation process in ALD[99] (Copyright (2009) Elsevier).

Comparing the original cathode surface to the ALD-coated ZrO_2, this reduction was observed. Moreover, the thermal accelerometer was created using plasma-enhanced ALD, which allows the creation of ultrathin materials platinum films with a better density and more stability and more stability.[101] The constructed accelerometer has reduced its cross section by 100 times, which has improved heating efficiency and assisted in lowering thermal time constants.

5.2 Etching

In ancient times, etching was a method for removing material from substrates by using the appropriate etchant. In the literature, numerous substrate–etchant combinations have been described that make etching a variety of substrates easier. Today, advances in conventional etching techniques like maskless etching and atomic layer etching (ALE) are based on evolving requirements. Reactive ion etching is a controlled etching method; ALE is a modified etching method. Essentially, this technique consists of two steps: (i) self-limiting modification, which changes just the top atomic layer of the substrate, and (ii) etching, which eliminates only the top layer. In continuous or pulsed plasma processes, this method might be used to address issues with aspect ratio, profile dependence, and selectivity. The ALE has long been a fascinating topic of study, even though silicon is the most commonly used substrate for MEMS devices. There have been several reports of using gas plasmas for silicon etching, including Ar/C_4F_8, Ar/CHF_3 and Ar/Cl_2.[102,103] These plasmas combine argon (Ar) with other gases. It has been possible to create both 2D trenches and 3D features using Ar/Cl_2 plasma. In every cycle, regulated pulse plasma produces a very effective etching at the atomic level. SiO_2 substrate can also be etched using a mix of Ar/Cl_2 plasma. In a plasma etching chamber, silicon nitride, another popular semiconductor substrate, has also been self-limited etched. The surface modification is self-limited using hydrogen plasma, and the etching is completed with fluorinated plasma. Fig. 4 illustrates the quasi-ALE of silicon nitride. Silicon is the most commonly used substrate for creating MEMS devices, so this ALE has long been a fascinating topic of study since it is anisotropic and selective for oxides (>100). In recent years, molybdenum disulfides (MoS_2) have received considerable attention. The bandgap varies from 1.29 to 1.9 eV depending on the number of layers (bandgap increases with decreasing layers). Thus, ALE is used to control the MoS_2 layers at the very beginning.[104] ALE reduces the thickness of MoS_2 while limiting contamination. As a result, it represents a method for the clean adsorption and desorption of reactive compounds. Additionally, the electrical properties of the material were noted etched surfaces stay close to those of the original surface when a mixture of low energy Ar radicals and chlorine radicals (Cl) is used as an adsorption and desorption reagent.

The other etching modification, called maskless etching, is likewise utilised to etch 3D structures in the silicon substrate in KOH. This approach has allowed the etching, which was originally limited to the (100) plane, to reach different planes. According to Li *et al.* the cutting planes for convex edges were {311}, while those for convex corners were {411}.[105] CMOS used for maskless etching of 3D MEMS structures on SOI (SiO_2 and SiN_2) dielectric membrane.[106] Because the designs are transferred using CMOS metallization layer-based microstructures, this approach does not require a specific mask.

5.3 Printing

On a paper substrate exclusively, MEMS-based force sensors are also developed using the basic screen printing process.[107] The conductive material—which is to be printed as ink—that is printed on the paper substrate produces a piezoresistive effect that powers these sensors.[108] It produced cantilever structures using Whatman chromatography paper, screen-printed carbon resistors (made with graphite ink), and contact pads made of silver ink. This method produces force sensors that can be utilised in two ways: one way is to put the printed sensors directly for an application, and another way is to fold the paper-printed sensors to use them in a three-dimensional setting.[108]

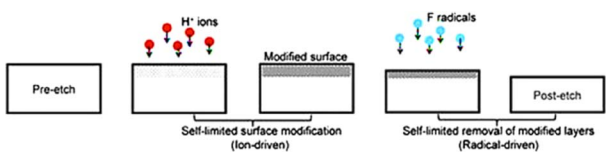

Fig. 4 Schematic view of a single silicon nitride quasi-ALE cycle[103] (Copyright (2017) AIP publishing).

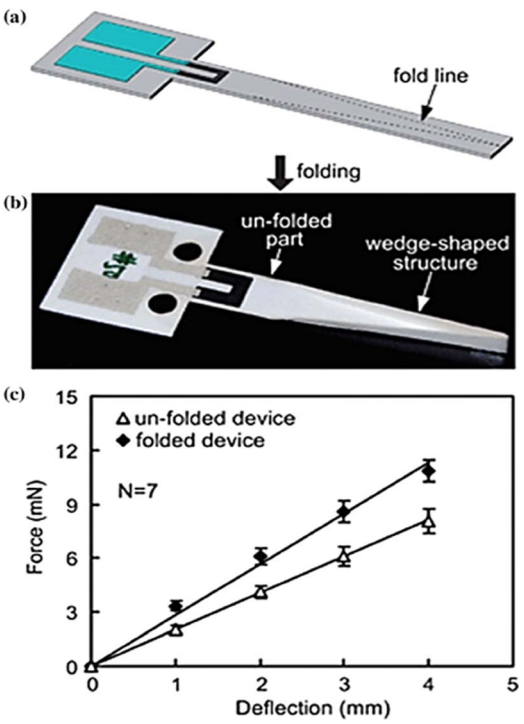

Fig. 5 Piezoresistive force sensor based on paper (a) schematic diagram of a paper-based force sensor with a laser-cut perforation of the fold lines and a carbon resistor (black) as the sensing element and contact pads with silver ink (blue); (b) the folded sensor; (c) folded and unfolded cantilever's force–deflection curve[107] (Copyright (2011) Royal Society of Chemistry).

Higher rigidity and sensitivity have also been demonstrated by the folded paper cantilevers depicted in Fig. 5.

6. Application

6.1 Display and touch screen

At this time, a wide range of sensing mechanisms for panels have been developed, including capacitive, acoustic wave, resistive, and infrared ray. Flexible touch panels have attracted a great deal of interest and are regarded as future electronic components because they offer a simple and intuitive interface for human–machine interaction. In recent years, flexible touch panels have attracted considerable attention because of their simple and intuitive interfaces for human–machine interaction. The present state of panel sensing technology includes capacitive, acoustic wave, resistive, and infrared ray sensing mechanisms. Using a lithium-containing polyacrylamide hydrogel, Kim *et al.* developed an ionic touch screen; the panel was elastic and soft and could withstand significant deformation (Table 2).[109] As part of their research, they also investigated the 1D ion touchpad's position sensor technology and used it to write letters on a 2D panel (Fig. 6(a)). There is no functional compromise when up to 1000% of strain is applied to the touchpad. The self-repairing man-touch pad interaction machine developed by Wang *et al.* consists of a soft, transparent, self-healing polyzwitterion–clay nanocomposite hydrogel with pressure-sensitive adhesion and high transmittance (98.8%) and fracture strain (1500%).[110] Capacitive technology senses touch position and can detect point-by-point touches and continuous movements (Fig. 6(b) and (c)).

6.2 Sensors

Sensors are devices that are designed to mimic the basic sensory functions of human sense organs, which can detect and respond to outside stimuli.[22,111] A sensor's primary function involves converting a physical or chemical stimulus into a different kind of energy.[112]

Since these sensors are in contact with the skin or tissues for a long period, they must be extremely flexible, soft, biocompatible, and nontoxic so they can be used safely and ergonomically.[113] The primary application of hydrogels in sensors involves signal detection from human tissues.

The use of hydrogel-based wearable sensors in medical diagnostics, biological signal detection, and other physiologically relevant applications is thought to play a significant role in the future. Unlike traditional sensors, hydrogel sensors rely more on the special characteristics of hydrogels, such as high-water content, stimulation responsiveness, and high permeability.[22] Depending on the requirements, different hydrogels can respond to different stimuli, such as temperature, strain, *etc.*

6.2.1 Temperature sensors. By using hydrogel-based temperature sensors, the temperature stimulus usually becomes a measurable physical response, whether geometric (Fig. 7(a)), optical (Fig. 7(b)), or electrical (Fig. 7(c)). Since hydrogels' conductivity is proportional to their ion mobility, their resistance is sensitive to ambient temperature and can be used to construct temperature sensors. As an example of a dynamic hydrogen-bonding network, Lei *et al.* created a type of resistive temperature sensor (Table 2) by using poly-zwitterionic poly(ammonium 3-dimethyl(methacryloyloxy ethyl) propane sulfonate) (PDMAPS), ion-rich 1-ethyl-3-methylimidazole ethyl sulphate (IL), and hydrogen-bond donor poly(acrylic acid) (PAA).[114] Due to hydrogen bonds, this design was able to overcome early electronic conductive materials' drawbacks that were sensitive to large deformations, while maintaining >95% resistivity stability under 1000% deformation. Generally, traditional conductive materials do not have such excellent mechanical properties, but this design also achieved high transmission of >90% and super tensile strains of >10 000%. Interestingly, Yu *et al.* a polyethylene glycol hydrogel, modified with Rhodamine B-embedded silicon nanoparticles ($RhB@SiO_2$) and gold nanorods (AuNR).[117] Under near-infrared laser irradiation, this composite hydrogel produced a three-dimensional temperature gradient through localized surface plasmon resonance of AuNR. As a result of the synergistic effects between AuNR and $RhB@SiO_2$ enclosed in hydrogels As a result of the synergistic effects between AuNR and $RhB@SiO_2$ enclosed in hydrogels, a temperature resolution of 0.74% per °C could be obtained (Fig. 7(d)).

6.2.2 Chemical sensors. By using hydrogel-based chemical sensors, chemical stimuli can be translated into changes in geometry and optics (Fig. 8(a)). The geometry of hydrogels changed as a result of volume variations in polymer networks in solution. Khademhosseini *et al.* have developed a simple and affordable method to incorporate mesoporous particles packed with fluorescent dyes into alginate hydrogel fibres using a microfluidic spinning system, which allows the colour changes to indicate changes in skin pH (Fig. 8(a)).[118] The hydrogel responds to pH values between 6.5 and 9. The technology will be able to monitor the pH in real-time and make an initial assessment of the wound healing. The PEDOT:PSS conductive hydrogel was developed by Xu *et al.* for the detection of urinary uric acid (Fig. 8(b)).[119] Fig. 8(b) shows that the sensor is constructed with a conductive hydrogel, which indicates high sensitivity and a detection limit of around 1.2 M (S/N = 3). Lee *et al.* developed a muscle-inspired MXene PAA/PVA hydrogel as a pH and strain sensor.[120] The pH level of sweating is measured using a hydrogel sensor, which to some extent reflects the level of fatigue in human muscles (Fig. 8(c)). As a result of the change in electrical resistance of the negatively charged surfaces of MXene, we were able to detect the pH variation in sweat. Fig. 8(c) shows the results of detecting pH between 3–6. Depending on the pH of the environment, MXene may have a stronger or weaker cation selectivity.

6.2.3 Gas sensors. In today's world, people are frequently exposed to unknown gases in their daily lives, and at work, they may even enter dangerous environments with irreversible consequences. The use of wearable and portable gas sensors helps mitigate this issue by accurately identifying hazardous gases that are difficult to distinguish, detecting risks, and steering clear of dangerous areas, protecting people from harm. Furthermore, wearable gas sensors are used in medical

Table 2 Some examples of hydrogel based flexible electronics and devices

Flexible electronics	Hydrogel	Activity	Requirements	Ref.
Touch screen	Polyacrylate, LiCl	An optical information-transmitting hydrogel ionic touch panel	Conductive and transparent	109
Temperature sensors	PDMAPS-IL-PAA	Ultra-stretchable (>10 000% strain); high-modulus (>2 MPa Young's modulus); healing; highly transparent (>90% transmittance); self-healing	Response of temperature stimuli and conductive	114
	PVA-DMSO	Temperature range (−30–60 °C); high toughness (3.1 MPa, 600%)		182
	N-Phenylaminomethyl POSS	Transmission modulated automatically upon environmental temperature shifts; high toughness and high stretchability (10 000% strain)		183
Chemical sensor	PEDOT:PSS	Ultrahigh sensitivity of 0.875 μm^{-1} cm^{-2} and a low limit of detection down to 1.2 μm	Response to pH, antigens and other chemicals; conductive	119
	MXene PAA/PVA	Change in electrical resistance of MXene negative charged surface allowed for the detection of the sweat pH alteration; pH range = 3–6	—	120
	PAAm–PAAc	Design a robust chemo-mechanical sorting system able to concerted catch and release of target biomolecules from a solution mixture		184
	Alginate-pH-responsive beads	Hydrogel microfibers containing mesoporous particles loaded with a pH-responsive dye		118
Strain sensor	Ionic polyacrylamide	High sensitivity of 2.33 kPa^{-1} with a capacitance sensitivity of 103.8 nF kPa^{-1}	Conductive	185
	PAAm–NaCl	Broad pressure detection range (≈35 Pa to 330 kPa), ultrahigh baseline of capacitance and fast response time (18 ms)		186
	PDA-clay-PSBMA	4.3 sensitivity; wireless transmission of signals captured by hydrogel sensors		187
	PEA-r-PS-r-PDVB [EMI] [TFSI]	High sensitivity of ≈152.8 kPa^{-1}, a broad sensory pressure range (up to 400 kPa), and excellent durability (>6000 cycles)		188
Gas sensor	S-rGO	Sensing concentration 4 and 20 ppm; LOD = 4.1 ppb and 1.48 ppm respectively	Response to wide range of NO_2, NH_3, CO_2, explosive *etc.* gas sensing; conductive	121
	SnO_2/rGO	Sensing concentration 5 ppm concentration; LOD = 2.8 ppm		122
	Functionalized-rGO	Device exhibits nearly twice as high response (1.65% response to 1000 ppm) with lower detection limit (20 ppm)		128
	Colorimetric reagents on the PDMS substrate	Sensing concentrations as low as 39.4 pg with a response time of about 0.2 s		130
Humidity sensor	Poly-carboxybetaine	Fast response (0.27 s), recovery time (0.3 s), and wide relative humidity detection range (4–90%)	Humidity sensing; conductive	180
	Gelatin, glycerol, chitosan, and sodium chloride	RH detection range of 20–90% and recovery time only 0.41 s		67
Tactile sensor	Sulfate/polyacryl–acrylamide (SA–Zn) hydrogel based TENG	Stretchability (>10 000%), excellent transparency (>95%), and good conductivity (0.34 S m^{-1})	Tactile sensing, ionic conductive	162
Energy storage devices	PANa	High cycling stability and capacities	Ionically conductive	180

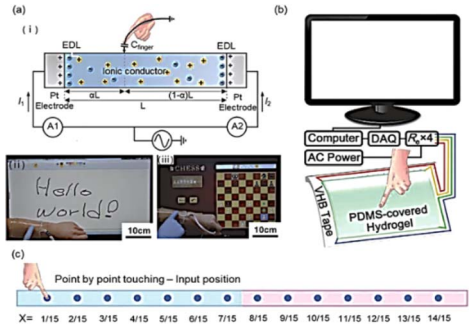

Fig. 6 (a) The touch strip architecture (i) motion detection capabilities of the epidermal touch panel; (ii) word writing demonstrations; (iii) chess playing[109] (Copyright (2016) *Science*). (b) Schematic illustration showed that a wearable touch pad gets integrated into a desktop computer; (c) corresponding V_1 voltage after touching each spot on the hydrogel strip with your finger[110] (Copyright (2020) *Advanced Materials*).

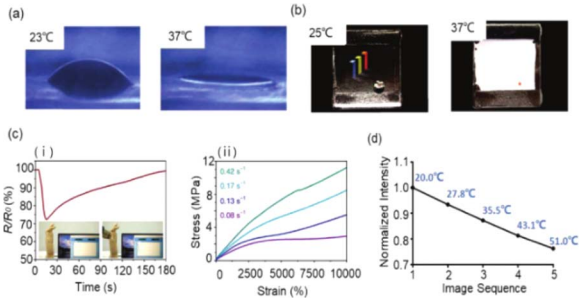

Fig. 7 (a) Temperature-sensitive hydrogels and exhibit geometrical response;[115] (b) thermal sensitive hydrogels that exhibit an optical response;[116] (c) (i) temperature variations in the surrounding air get identified by the sensor through resistance signals (ii) conductive hydrogel showed a tensile strain around 10 000% that was extremely long;[114] (d) within the temperature range, the fluorescence intensity of RhB@SiO_2 particles linearly correlated with room temperature[117] (Copyright (2006) *Nature*); (Copyright (2019) *Joule*); (Copyright (2019) *Nature Communications*); (Copyright (2022) *Adv. Funct. Mater.*).

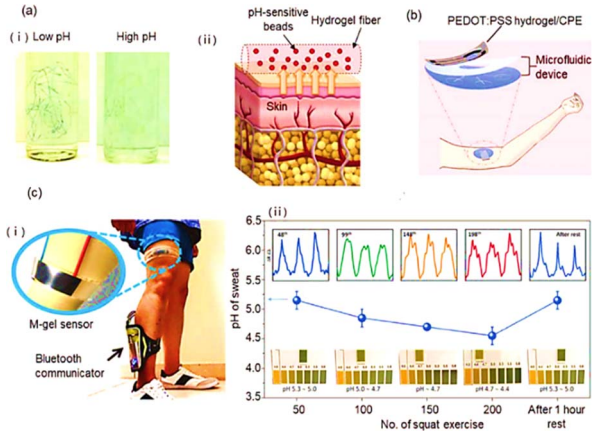

Fig. 8 (a) (i) pH responsive bead-laden hydrogel microfibers, (ii) pH sensing hydrogel microfibers for epidermal monitoring; (b) schematic view of wearable uric acid sensor; (c) (i) wireless hydrogel sensor used for detection of muscle fatigue *via* pH detection, (ii) resistance changes measured over different number of movements[5] (Copyright (2023) *Advance materials*).

applications for diseases like asthma. Current gas-sensing applications include NH_3, NO_2, O_2, and CO_2 using hydrogels. To achieve real-time and reliable monitoring of the concentration of target gases at room temperature, hydrogels exhibit flexibility and stretchability, making them suitable for this application.

Compared to conventional gas sensors based on semiconductors and electrochemistry, conductive hydrogel-based gas sensors are relatively new. In Fig. 9(a)(i), a basic gas sensor is formed by inserting one electrode at the ends of a hydrogel. An electrochemical sensor based on hydrogels can be very useful in the field of gas detection. Hydrogel-based gas sensors currently focus on NO_2 as one of the most studied gases. As an electronically conductive hydrogel material, rGO is ideal for gas sensing because of its wide specific surface area and three-dimensional porous structure. According to Wu *et al.*, reduced graphene oxide hydrogels have been modified with $NaHSO_3$ and a S-rGO-based hydrogel has been synthesized. Using reduced graphene oxide hydrogels modified with $NaHSO_3$ and synthesized with S-rGO-based hydrogels, they developed a gas sensor that can detect NO_2 and NH_3 in real-time.[121] In comparison with the unmodified device, S-rGO hydrogel was 58.9 and 118.6 times more sensitive. Therefore, the material composition of the sensors should be biocompatible, non-toxic, and environmentally friendly for the applications of wearable and portable gas sensors. To improve the selectivity of hydrogel-based gas sensors for NO_2, Wu *et al.* synthesized a three-dimensional graphene hydrogel modified with SnO_2 (SnO_2/r-GO), which has a high sensitivity of 4.3 ppm^{-1} at room temperature and a very low theoretical detection limit of 2.8 ppm.[122] Additionally, Fig. 9(a)(ii and iii) showed, the improved conductivity of the material resulting from the existence of the p–n junction between rGO and SnO_2, and the sensitivity of the NO_2 device increased considerably boosted the selectivity of the sensor for NO_2. Wu *et al.* developed a salt-infiltrated hydrogel that allows for real-time NO_2 monitoring at room temperature.[123] By adding $CaCl_2$ to the PAM/Carr DN hydrogel using a straightforward solution infiltration method. Result, it had an NO_2 sensor with a high sensitivity of 119.9%, a short response and recovery time (29.8 and 41.0 s, respectively), good linearity, a low theoretical limit of detection (LOD) of 86 ppt, high selectivity, stability, and ionic conductivity. As shown in Fig. 9(a)(iv), the sensor is self-healing recovers after being truncated, and retains its conductive and sensitive properties. They also developed a novel self-powered flexible NO_2 sensor based on the structure of Zn-zinc trifluoromethane sulfonate ($Zn(OTf)_2$)/PAM hydrogel-carbon (Fig. 9(a)(v)).[124] The sensor had extremely high sensitivity (1.92% ppb^{-1}), a very low theoretical LOD (0.1 ppb), and excellent NO_2 selectivity. It works even in extreme conditions such as stretching, bending, sub-zero temperatures, and high humidity.

Liu *et al.* developed a highly sensitive, nontoxic, and environmentally friendly electrical NH_3 hydrogel sensor from

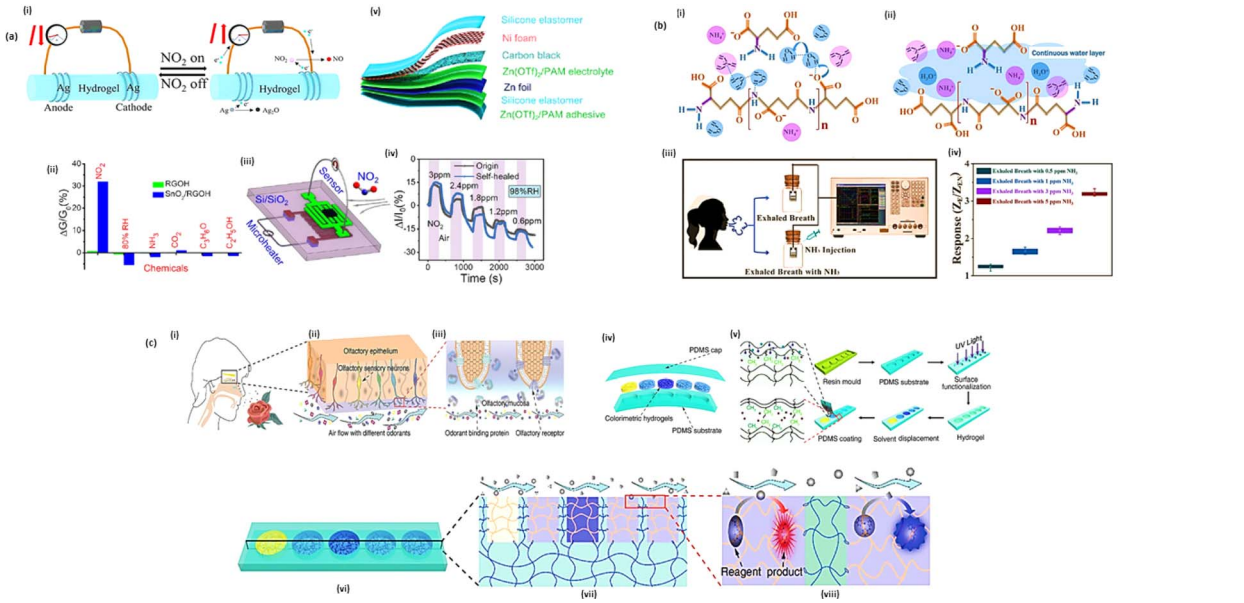

Fig. 9 (a) Hydrogel based NO_2 gas sensor (i) schematic diagram of gas sensing process through hydrogel based gas sensor. For NO_2 gas (ii) schematic diagram of SnO_2/rGO hydrogel selectivity. (iii) Schematic diagram of microheater device used in sensing process. (iv) Comparison in between self-healing hydrogel's response capacity and the original hydrogel's response capacity for NO_2 gas. (v) Design of self-powered NO_2 sensor; (b) hydrogel based NH_3 gas sensor (i) sensing mechanism of PGA/GA sensor at low RH value (ii) sensing mechanism of PGA/GA sensor at high RH value. (iii) Schematic diagram of breath testing process for NH_3 gas. (iv) Hydrogels' reaction to exhalation with varying NH_3 concentrations; (c) hydrogel based explosive gas sensors. (i–iii) An illustration of the human olfactory system used to transmit olfactory signals (iv and v) Structure and fabrication for colorimetric hydrogel sensor. (vi–viii) Demonstration of colorimetric hydrogel sensor's sensing procedure on the target material[131] (Copyright (2023) *Nano-Micro Letters*).

biomass hydrogel GA and poly-L-glutamate (PGA) composite materials.[125] At 80% relative humidity, the sensor was able to detect NH_3 up to 50 parts per million with a LOD as low as 0.5 parts per million and good NH_3 selectivity. It is primarily due to the synergistic effect between PGA and GA that PGA/GA exhibits high response performance (Fig. 9(b)(i and ii)). Due to their similar chemical structures, PGA and GA had excellent chemical compatibility. We aim to develop a high-sensitivity, high-selectivity NH_3 gas sensor using CA/PEGDA hydrogels (80% relative humidity). In Zhang *et al.* study, citric acid (CA) was encapsulated into PEGDA hydrogels using thiolene photochemistry.[126] The sensor measured a high response (6.20) and minimal LOD (50 ppb) at room temperature. According to Fig. 9(b)(iii and iv), this sensor is capable of precisely measuring NH_3 levels in exhaled air. Exhaled human breath was also tested for NH_3. Whenever carbonaceous materials burn, CO_2 is created as a byproduct of respiration. The production of CO_2 by organisms will continue if they breathe. Wang *et al.* achieved fast, real-time, and continuous monitoring of dissolved CO_2. An *in situ* Schiff base reaction was used to make hydrogel membranes from branched polyethyleneimine (BPEI) and partially oxidized dextran (PO-DEX).[127] When CO_2 is added to react with the amino group in BPEI, the BPEI/PO-DEX films swell in water. To detect dissolved CO_2, the Fabry–Perot stripe on the reluctance spectrum of BPEI/PO-DEX film is used as a sensing signal. To achieve high-performance CO_2 sensing, Wu *et al.* developed a hydrogel material that responds directly to CO_2 gas.[128] Through a straightforward one-step hydrothermal method, they produced 3D chemically functionalized reduced graphite oxide hydrogels (functionalized – rGO hydrogels) using hydroquinone molecules. There is a nearly double response to CO_2 in the functionalized – rGO hydrogel sensor (1.65% response to 1000 ppm CO_2) with a lower detection limit (20 ppm) than the unmodified rGO hydrogel sensor. CO_2 adsorption on the hydrogel surface results in a lower rGO fermi energy level than the highest occupied molecular orbital (HOMO). Charges are transferred from CO_2 to rGO orbitals through hybridization, increasing rGO charge (hole) concentration and decreasing hydrogel resistance. Hydrogel devices with higher initial resistance had a broader response space, which resulted in higher reactions; however, this hydrogel CO_2 sensor was temperature-sensitive, and increasing temperature would cause a decrease in response.

In several countries and their citizens, explosive-based terrorist attacks have caused public safety problems. Exposure to explosives for a long or short period may also cause damage to human health. Typically, explosives are very sensitive. Hence, it is critical to develop sensing devices that can detect explosives quickly, sensitively, accurately, and without contact.[129] Wang *et al.* A multifunctional hydrogel detector mimics the human olfactory system and can detect a wide range of explosive compounds (Fig. 9(c)).[130] According to Fig. 9(c), they mixed hydrogels with colorimetric reagents and developed hydrogels *in situ* after applying colorimetric reagents to the PDMS substrate. After the target microparticles are delivered and adsorbent by hydrogel, colorimetric reagents are used to mimic odor-binding proteins (Fig. 9(c)). As a result, the hydrogel sensor had a response time of approximately 0.2 s and

a detection limit as low as 39.4 pg. In ambient temperatures, it was able to distinguish five basic igniters, including hypochlorite, chlorate, perchlorate, urea, and nitrate. A variety of basic explosives were marked with different colours, and the shade of colour indicated the concentration of the target gas.

6.2.4 Strain sensor. To create a capacitive hydrogel stress/strain sensor, a dielectric layer is sandwiched between two hydrogel layers. A change in the distance between the two hydrogel layers is most likely caused by an external force, and adjusting the contact area between the hydrogel and the dielectric will change the capacitance, which can then be measured to determine stress/strain. First, Suo *et al.* developed an electronic skin that can be used as a strain/strain sensor (Fig. 10(a)). Ionic skin sensors detected pressing positions as well as the pressure of mild finger touches (10 kPa).[132] A series of lithium-ion micro batteries, solar cells, and MXene hydrogel as a pressure sensor was used by Zhang *et al.* in an all-flexible, self-powered integrated system.[133] A pack of 100 MXene-based micro-supercapacitors connected in series generates the highest voltage output for MXene-based micro-supercapacitors currently, which is 60 V (Fig. 10(b)). Sheen *et al.* developed a robot prosthesis that has tactile sensing and functions as a capacitive pressure sensor using a robot prosthesis that responds to body movements in 35 ms.[134] With the help of conductive textiles and PAAm–NaCl hydrogel, this pressure sensor was developed using a simple fabrication process. In Fig. 10(c), the pressure sensor has ultrahigh capacitance and sensitivity, while its response time (18 ms) is much faster than human skin (40 ms). A variety of stimuli-responsive hydrogels were developed by Guo *et al.* By adding conductive materials to PNIPAM, they made hydrogels that were biocompatible and detected joint bending signals.[56,135]

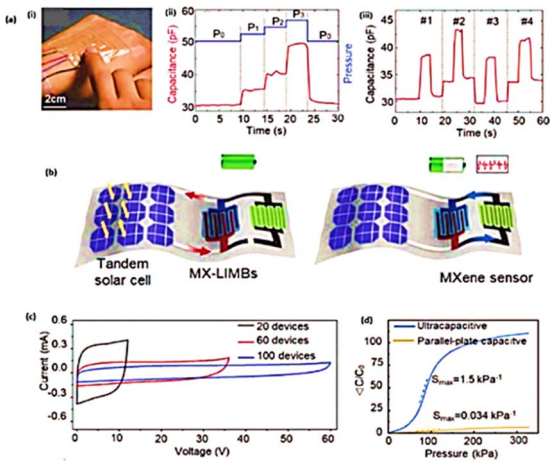

Fig. 10 (a) (i) Strain sensor attached back of the hand. (ii) Sensor detect the pressure of touch. (iii) The sensor's location of the touch; (b) schematic diagram of the charging and sensing of an MXene-based all-flexible, self-powered integrated pressure sensing system.; (c) CV curves for a tandem MXene micro-supercapacitor with 20, 60, and 100 cycles; (d) pressure sensitivity comparison of the conventional parallel plate capacitive sensor and the ultra-capacitive ionotropic pressure sensor[5] (Copyright (2023) *Advance materials*).

Using the relationship between hydrogel resistance and mechanical deformation, a hydrogel resistance strain sensor was developed. Zheng *et al.* developed a zwitterionic hydrogel using 3-(1-(4-vinylbenzyl)-1*H*-imidazol-3-ium-3-yl)propane-1-sulfonate as monomer.[136] The hydrogel had a fracture stress of 200 kPa and a fracture elongation ratio of around 4.5, making it suitable for use as a strain sensor. With the addition of benzene and imidazole groups, the polymer-rich phase's increased chain stiffness, interchain contacts, and associative strength, as well as its microphase-separated structure, led to improved mechanical properties for the hydrogel. Compared to the standard zwitterionic hydrogel, stretchability and fracture toughness were increased by 40 and 60 times, respectively. Using microphase separation of plastic elastomers and physical crosslinking, Cai *et al.* developed acrylonitrile copolymer hydrogel as strain sensor.[137] Acrylonitrile copolymer hydrogel has a maximum fracture energy of approximately 7592 J m^{-2}, and it will be treated cyclically. A dual-channel hydrogel flexible strain sensor has been developed by Lin *et al.*[138]

As shown in Fig. 11, the strain sensor transformed into optical and electrical information. Films of polydimethylsiloxane and carbon nanotubes make up the sensor. Using carbon nanotube films, stretch-induced network microcracks can be precisely controlled, allowing simultaneous output of electrical and optical signals output of electrical and optical signals.

6.2.5 Mechanical sensor. Intelligent flexible mechanical sensors are intended to identify physical parameters. A popular sensing mechanism which based on geometry deformation of sensing element under external mechanical forces and able to translate into an electrical signal for detection.

For sensitive and quick response to pushing or stretching, a variety of sensory devices that are sensitive to deformation under mechanical forces have been developed. As sensing elements in mechanical sensors, conductive hydrogels, created by adding conductive fillers to hydrogel matrix, have been used in robotics, medicine, and wearable health monitoring as part of integrated multisensory systems.[139–141] As fillers, conductive polymers and carbon components were frequently used to produce conductive hydrogels that were extremely flexible and sensitive because of their high electrical conductivity. As a result of external forces, these sensors typically detect changes in resistance resulting from changes in shape. Zhang *et al.* fabricated a force-sensitive, conductive hydrogel by polymerizing aniline and AAM in a colloid with swelling chitosan

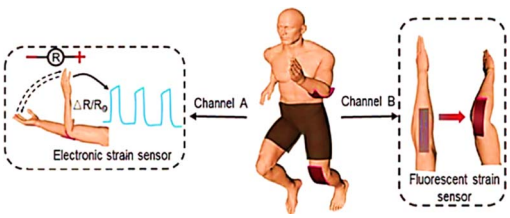

Fig. 11 Schematic demonstration of two-way electronic and fluorescent colour reactions to motion in humans[5] (Copyright (2023) *Advance materials*).

microspheres.[142] Chitosan microspheres are evenly distributed throughout the hydrogel and act as microscale connections for improved energy dissipation and strength, giving the hydrogel super-stretchability (strain exceeding 600%), high strength, and exceptional mechanical stability. In addition, the tough microspheres continuous phase PAAm/PANI caused a surface self-wrinkling structure that resulted in excellent force sensitivity. Resultant, the conductive hydrogels able to detect forces over a range of 100 Pa to several MPa with excellent electrical stability and rapid response times (Fig. 12(a)). A highly sensitive, self-healing, mechanically adjustable, and capacitive ionic skin sensor was recently created with a bioinspired mineral hydrogel composed of tiny calcium carbonate nanoparticles and crosslinked polyacrylic acid.[143] Fig. 12(b) depicts the mineral hydrogel's schematic composition and measurement results. Because of the distinct viscoelastic behaviour of the resulting hydrogel, the hydrogel-based capacitive sensor possesses a high sensitivity to pressure and able to detect the smallest changes in pressure, like finger motion, a light touch, motion in the throat, tiny water droplets (which mimic rain), and blood pressure. When damaged, the sensors self-healing abilities might restore them to their former conditions, giving them greater longevity and durability. A wearable, human-motion soft sensor that can heal itself and designed for healthcare monitoring.[144]

The sensor consisted a conductive hybrid network hydrogel that developed by dynamically cross-linking conductive functionalized single-wall carbon nanotubes, PVA, and PDA. It allowed for easy breaking and re-bonding of cross-linking, which provided conductive hydrogels the ability to heal themselves (Fig. 12(c)).

6.2.6 Tactile sensor. An adaptive tactile sensor will be able to sense pressure, touch, and other physical interactions more instinctively and naturally thanks to its ability to bend and change with the surface.[145–147] Flexible tactile sensors have gained significant attention from scientists lately since they can enhance emerging human interaction technologies, such as artificial skin-like sensors, wearables, and user-interactive devices.[148] Adding conducting elements to hydrogel matrices can create conductive hydrogels, one of the best materials for the construction of flexible tactile sensors. In order to create electronic conductive hydrogels, different electronic conductive materials have been embedded into hydrogel matrix, such as conductive polymers, metal nanoparticles/nanowires, liquid metals, MXenes, and carbon-based compounds.[149–154] Recently, ionic hydrogels have been developed for tactile sensors, which typically use two kinds of conventional sensors. With a resistive- or capacitive-based sensor, variations in electrical properties of resistors and capacitors can be translated into variations in external mechanical stimuli. In order to create a flexible sensor that can bend, press fingers, and measure carotid pulses, a micro structured electrolyte and double-layer capacitors were used. Yang *et al.* developed a wearable resistivity sensor using a chitosan-poly(hydroxyethyl acrylamide) double-network hydrogel that is robust, anti-fatigue, and freezing-tolerant.[155] A tactile sensor that is flexible could be used to detect mechanical stimuli that are stationary or change gradually. Through the processes of contact electrification and electrostatic induction, triboelectric nanogenerators (TENGs) could convert ambient mechanical energy into useful electricity.[156] Through the regeneration of chemically cross-linked cellulose, Hu *et al.* produced transparent, conductive, and flexible cellulose hydrogels in an aqueous solution of NaCl.[157] For the first time, Xu *et al.* created a PVA hydrogel-based triboelectric nanogenerator (hydrogel-TENG) device that can function as a self-powered sensor to identify human motions.[158]

The cellulose hydrogel had excellent mechanical properties (tensile strength and elongation at break of 5.2 MPa and 235%), conductivity (4.03 S m^{-1}), transparency over 94% at 550 nm, and low-temperature tolerance down to −33.5 °C were largely influenced by the presence of NaCl in the hydrogel matrix. A cellulose/NaCl hydrogel (CNH) sample was encased between two VHB layers. An exterior triboelectric layer made of latex was employed (Fig. 13(a)(I)). To build a self-powered tactile/pressure sensor with a sensitivity of 0.0068 kPa^{-1} and a pressure detection limit of around 0.392 kPa, the cellulose hydrogel-based triboelectric nanogenerator was coupled to an external load of 220 MΩ (Fig. 13(a)(II and III)). The TENG sensor, that was based on cellulose hydrogel, demonstrated remarkable properties such as conductivity of 0.72 S m^{-1}, elongation at break of 220%, outstanding tensile strength of 6.8 MPa, and high optical transmittance of 97% at 550 nm. Further, it had a pressure sensitivity of 0.0103 kPa^{-1} and a pressure detection limit around 16.8 Pa.[161] A hydrogel-based TENG was created by Lu *et al.* to track driver fatigue.[159] The driver's skin served as the second electric material for the hydrogel-based TENG, which was attached to her skin and operated in a single-electrode mode. Three characteristics were used to detect driver fatigue: the length of blink intervals, the percentage of time that eyelids are closed, and the frequency of yawning, all of which were compared to predefined thresholds. Another way to give the driver a timely notice was to use the blink length (Fig. 13(b)). A double-network polymer ionic conductor sodium alginate/zinc sulfate/polyacryl–acrylamide (SA–Zn) hydrogel was used by Sheng *et al.* to develop a TENG.[162] This hydrogel demonstrated exceptional stretchability (>10 000%), excellent transparency

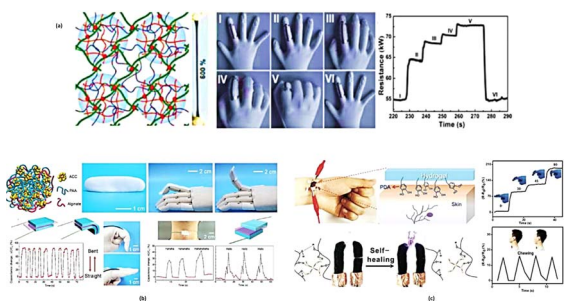

Fig. 12 (a) While a human hand grasps something, the MC-Gel, an electronic skin, is attached on the forefinger to track the movements and changes in resistance that result; (b) the ACC/PAA/alginate mineral hydrogel's schematic structure and sensor capabilities; (c) hydrogel-based hybrid network soft human-motion sensors could self-assemble, self-heal, and self-adhere to the wrist during healthcare monitoring and human–machine interaction[25] (Copyright (2018) *Chemistry–A European Journal*).

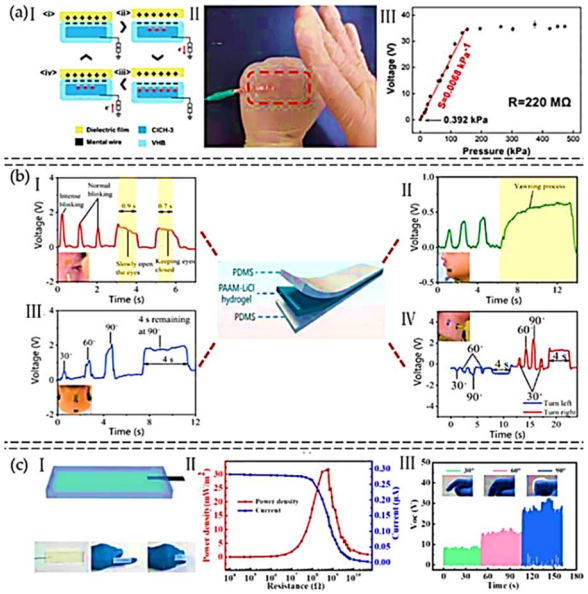

Fig. 13 (a) Cellulose based hydrogel for flexible sensor; (I) schematic view of CNH TENG mechanism; (II) finger-tapped translucent hydrogel TENG; (III) fluctuated pressures applied and corresponding peak voltage amplitudes across the resistor (220 MΩ).[157] (b) Driving fatigue monitoring with a hydrogel-based TENG; detection of (I) eye closure movement; (II) yawning; (III) head turning movement; (IV) vertical bending angle.[159] (c) Self-contained arm workout band sensor; (I) diagrammatic representation of SA–Zn hydrogel TENG and images of the SH-TENG folded and in its original form; (II) performance output of SH-TENG; (III) voltage outputs of the SH-TENG while the finger is bent[160] (Copyright (2021) *Carbohydrate Polymers*; Copyright (2020) *Nano Energy*).

(>95%), and good conductivity (0.34 S m^{-1}). By encasing the SA–Zn hydrogel in ecofilm films, the SA–Zn hydrogel TENG (SH-TENG) was created (Fig. 13(c)(I)). At an external resistance of 0.6 GW, the SH-TENG's power density can reach a maximum of 32 mW m^{-2} (Fig. 13(c)(II)). By enclosing the SA–Zn hydrogel in silicone rubber to create a sealed sandwich structure, the self-powered sensor was put together. The SA–Zn TENG's potential as a smart arm training band sensor for real-time monitoring was indicated by the output voltage's direct linear correlation with the applied force (Fig. 13(c)(III)). Although stretchable hydrogels can naturally stretch and therefore preferred signal carriers for biological areas, ionic conductors based on these materials become growing in significance in the development of wearable technology. Li *et al.* described tactile sensors which constructed from a hydrogel of poly(acrylamide)/poly(ethylene oxide)/LiCl.[163] These hydrogels had excellent mechanical properties, including high stretchability (approximately 8.8 times, 100 mm min^{-1}), high compression strength (556.58 MPa), high stabilises and damage resistance, and nearly 100% electrical self-healing ability, due to their chemically crosslinked structures and multiple H-bonding networks. The hydrogels have an ionic conductivity of around 8 S m^{-1} due to the usage of salts (LiCl) as conductive ions. It proved that the ionic conducting hydrogels could monitor both external pressure and human activity as very sensitive strain/tactile sensors. These hydrogel-based ionic sensors could be used in soft robotics, human/machine interfaces, and sports monitoring. Chun *et al.* developed T-skin films employing conductive piezoresistive and piezoelectric particles in an elastic polymer matrix to produce stretchy artificial skin that can resemble biological tactile mechanoreceptors. $BaTiO_3$ nanoparticles, which have an average diameter of approximately 30 nm, are encircled by high-aspect-ratio plate-type reduced graphene oxide (rGO) sheets, which have an average lateral particle dimension of approximately 20 μm and thickness of approximately 1–1.4 nm. The materials are evenly dispersed within a polydimethylsiloxane (PDMS) polymer matrix (Fig. 14(a and b)). For a passive body skin system, the T-skin film can be used as a sensor (Fig. 14(c)). A T-skin device linked to human or robotic skin is stimulated by a pressing stimulus within the range that human glorious skin can detect (Fig. 14(d)). Static pressure does not affect the FA sensor (Fig. 14(f)), but it does affect the SA sensor (Fig. 14(e)). The SA and FA sensors demonstrate consistent piezoresistive and piezoelectric responses while exposed to pressure (0.1–100 kPa, which corresponds to the typical human pressure perception range 2). It is interesting to note that the FA sensor can detect high-frequency vibrations (1000 Hz), which is higher than the maximum 500 Hz vibration detection range for humans (Fig. 14(g)).[147,164] An individual sensory neuron receptor in the human body called a nociceptor is able to recognise signals that are damaging and cause the central nervous system to trigger a muscular response.[165] Khan *et al.* firstly described, a nickel-doped zinc oxide (NZO)/Au based memristor is created

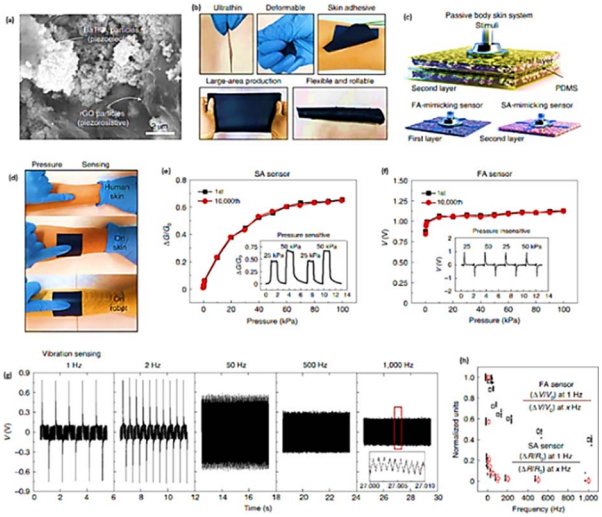

Fig. 14 (a) Scanning electron microscope image of T-skin film; (b) ultrathin, lightweight, deformable, adhesive T-skin film; (c) T-skin sensor arrangement for body skin system passiveness; (d) with real human skin, T-skin sensors on human skin, or robotic skin passive body skin gets subjected to a driving stimulus; (e) SA sensor; (f) FA sensor; (g) the FA sensor can detect vibrations at a frequency between 1 and 1000 Hz, which is higher than the human vibration detection range of 500 Hz; (h) FA sensor can detect vibrations at a frequency between 1 and 1000 Hz, which is higher than the human vibration detection range of 500 Hz.[147] (Copyright (2021) *Nature Electronics*).

and characterised for use in artificial nociceptor applications.[166] To reduce the NZO layer's surface effects and enhance volatile threshold switching performance, a nickel-doped zinc oxide (NZO) layer is positioned between the P++–Si and Au electrodes. For use in artificial intelligence systems, such as neural integrated devices with nanometre-sized features, this type of NZO-based device generates a crucial multifunctional nociceptor performance.[166]

6.3 Memristors devices

For data-driven computing and data storage, rapid advances in information technology have led to the investigation of scalable and high-speed memory devices. As a result of its straightforward two-terminal topology, resistive switching random access memory (RRAM) has low power consumption, low cost of manufacture, fast program/erase speed, and high density, making it a common form of memristor. Various strategies can be used for storing and processing data in a single unit, including processing with memory (PwM), processing in memory (PiM), and processing near memory (PnM).[167] The best singularity in memory processing is the storage device that serves as a processing unit. In memory, the storing and processing units are technically separate, but the processing element is united. Close to memory, the processing unit is located next to the memory unit rather than inside it. Researchers have shown considerable interest in memory processing out of the three methods. Therefore, emerging gadgets with both processors and non-volatile memory are extremely demanding. Fig. 15 illustrates the extensive research conducted on a few non-volatile memories, including resistive random access memory (RRAM), magneto resistive random access memory (MRAM), ferroelectric random access memory (FRAM), phase-change random access memory (PRAM), and resistive random access memory (RRAM).[169,170] Because of their improved features—such as lower energy consumption, a simple structure, the ability to store data in various states, a shorter data access time, and the possibility of three-dimensional (3D) integration—non-volatile emerging memory devices are displacing conventional memory devices.[171–173] Luigi Colombo proposed the implications of non-volatile developing memory technologies for memristive synapses. The concept of memristive synapses is a novel one in the field of computers inspired by the human brain. A cutting-edge gadget mimics the flexible and adaptable behaviour of biological synapses. The concept of resistive switching (RS) is a new technology that combines data processing and storage in a single cell. RS occurs when certain materials undergo periodic changes in electrical resistance in response to external electrical stimuli. Chua demonstrated that RS devices were actually memristors. Due to their ability to memorize historical data, RS devices are called memristors. In actuality, the terms “memory” and “resistor” are shortened to form the term “memristor”. As a result of the RS phenomenon first reported by Hewlett-Packard Laboratories, unconventional memories are being explored as a replacement for or to balance out the partial adaptability of silicon-based conventional memory technologies such as DRAM, SRAM, and Flash (NAND). In addition, a growing performance gap between cutting-edge technology and conventional memory compromises the potential for developing innovative memory devices. A unique non-volatile memory device has been explored using RS-based nanoscale memories (non-charge based); therefore, switching from charge-based storage to RS storage is a possible upgrade. This progression has been achieved through the development of a variety of concepts and storing mechanisms. These devices provide compensations in terms of switching speed, scalability, and cell area. Among those proposed are the spin-transfer torque memory (STTRAM), the phase change memory (PCM), and the RS memory (RRAM).[174–176] It is necessary to introduce parameters, which are primarily used to assess the performance of RS devices, before choosing the materials for RS layers. Materials such as transition metal (binary) oxides can be used as resistive layer materials or storage media based on their scalability, cost, consistency, energy consumption, and switching speed. Among the complex oxides are chalcogenides (such as sulphides, tellurides, and selenides), nitrides, complex oxides/perovskites, nonmetal elements, polymer organics (such as poly(methyl methacrylate), poly(*N*-vinyl carbazole), and polyaniline).[177] A number of complex oxides have high dielectric constants, including silk fibroin, albumen, nanocellulose, and bovine serum albumin. There are a wide variety of functional materials that exhibit RS behaviour, including ferromagnetic, dielectric, ferroelectric, and semiconducting materials. In order to create a higher grade film with highly oriented growth and fewer native defects, controlled film growth is required. The smooth deposition of the insulating coating was crucial to removing cell-to-cell variability. MIM structures were used in the material demonstrating RS capability, which were sandwiched between two electrodes (similar to a capacitor in a two-terminal configuration), as was described earlier. As part of the traditional fabrication method, the bottom electrode is first deposited on the substrate, and then an insulating layer is applied to the whole outside of the BE (bottom electrode). Finally, TE electrodes with the appropriate area can be placed over the insulating layer. The methods for deposition usually based on two approaches: (a) physical deposition, like electron beam evaporation, sputtering, thermal evaporation, pulsed-laser deposition, and electro-hydrodynamic printing, or (b) chemical transformation, like plasma enhanced molecular beam epitaxy, atomic layer deposition (ALD), rapid thermal oxidation, ultrasonic spray, pyrolysis, and the sol–gel process. It is still appropriate to use sputtering and atomic layer deposition with sputtered films at roughness level of 1 nm for RS

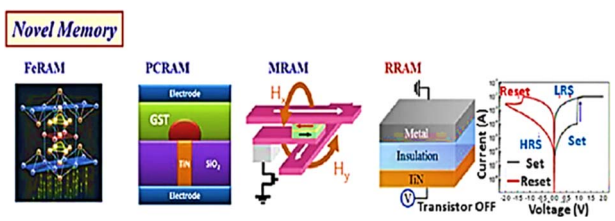

Fig. 15 Non-volatile memory devices, such as MRAM, PCRAM, and FeRAM[168] (Copyright (2016) *Materials Today*).

applications. Because sputtered RS media have a higher density of defects, they sometimes perform better than ALD media in RS.

Since its high resolution and chemical homogeneity make it possible to insert chemical dopants and regulate oxygen vacancy concentrations, ALD technology is gaining more attention for selective modification of the material composition. Despite this, various investigations have shown that ALD films lack RS;[178] whereas sputtered films have stable RS without annealing. Furthermore, sputtering has a simpler stoichiometry control process than ALD. For large-area uniform thin film deposition, radio frequency (RF) sputtering is the most popular method because of its low operating costs, nanoscale-controlled thickness regulation, and high yield.

6.4 Energy storage devices

In recent years, wearable electronics have gained a lot of attention due to their technological advancements, particularly in terms of their energy source. By introducing new functions into existing hydrogels, hydrogels can be transformed into unprecedented energy storage devices with additional functions through a highly abundant and tuneable chemistry. A typical electrochemical energy storage device consists of two electrodes and an electrolyte between them.[179]

Electrochemical capacitors store charge by adsorbing and desorbing electrolyte ions on their electrode surfaces. A new electrolyte made from sodium polyacrylate hydrogel (PANa) and a rechargeable zinc–air or Zn//NiCo battery have been described by Huang *et al.* (Fig. 16).[180] In each case, the electrolytes showed ultra-long cycle stability (16 000 cycles, 65% capacity maintenance, 800 cycles for 160 h), which was significantly better than the best solid-state equivalent.

A supercapacitor stores electrochemical energy by adsorbing electrolytic ions on its surface. Hydrogels serve as electrolytes in capacitors. In comparison to traditional capacitors, supercapacitors have higher capacitances, and their storage capacity can reach Farad levels.[181] Qin *et al.* developed an integrated charging energy storage system that consists of a thermoelectric generator (TENG) and a super-capacitor.[181] The hydrogel exhibited a 93% light transmittance, 1.92 S m^{-1}, and the ability to function normally at −54.3 °C. Under extreme conditions, the system can harvest and store energy, making it an ideal power source for wearable electronics.

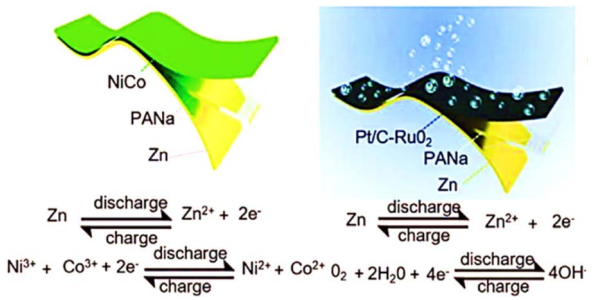

Fig. 16 Zn anode, NiCoOH cathode, and PANa polyelectrolyte composed the Zn//NiCo battery[180] (Copyright (2018) *Advanced Energy Materials*).

7. Conclusion and future prospects

During the last two decades, conductive and flexible hydrogels attracted significant interest due to the rapid development of flexible electronics, which improves our daily lives as well as protects us from disease. Incorporating conducting polymers, metal nanoparticles, and carbon-based nanomaterials into a flexible polymer network provides the foundation for electron-conductive hydrogels. The purpose of this review was to highlight and discuss current developments in flexible electronics based on hydrogels, with an emphasis on applications such as displays and touch screens, temperature sensors, chemical sensors, strain sensors, humidity sensor, tactile sensor and energy storage devices. Typically, hydrogels have low conductivity, making it difficult to directly print circuits on them. Conductivity of hydrogels has been enhanced through the addition of conductive dopants, the use of conductive polymers, and the implementation of double networks. A major challenge for the development of hydrogel-based flexible electronics is the mechanical weakness of the materials. Several strategies have been adopted to overcome it, including the use of anisotropic material, adding dopants, adopting an efficient energy dissipation platform, and incorporating hybrid systems. The ability for electronic skin settings to heal itself has been studied in many ways to determine how they can achieve this goal. A final problem is adherence of hydrogel to other materials, which is caused by the evaporation of water over time, gradually changing the properties of the hydrogel. The long-term water stability and environmental resistance of hydrogel-based flexible electronics present challenges. Encapsulating the hydrogel with elastomers and adding humectants may help resolve the adhesion issue.

Creating smart, small, integrated, flexible, and wearable devices require the integration of wireless circuits and sensor chips. At present, hydrogel-based sensors operate at a macroscopically visible level, preventing their miniaturization and large-scale integration. There is no unified set of standards for the preparation process of hydrogel-based gas and humidity sensors, so it has been difficult to exclude the effects of various preparation methods on the gas and humidity sensors. As a result, commercial applications of hydrogel-based gas and humidity sensors have been hindered. The development of hydrogel-based gas sensors requires further research into size reduction, uniform preparation, and hydrogel design for simple integration in dependent sensing systems. The great structural closeness of ionic hydrogels to natural soft tissues and their design flexibility have attracted significant interest in the fields of health monitoring and human–computer interaction. We have presented the research development on self-powered ionic hydrogel sensors in recent years. Ionic hydrogels have been used to create touch sensors, giving them a broad operating range and exceptional stretchability. In addition, ionic hydrogel technology-based structural design and performance optimization can lead to the creation of a high-performing tactile

sensor. Generally speaking, flexible conductive hydrogel electronic devices will be defined by cheap cost, high functionality, and stability. E-skin technology will be useful in both business and daily life as self-powered ionic hydrogel sensors grow swiftly and become integral to the next generation of electronic devices. As well as, wireless communication technologies progress, such as advanced Bluetooth and NFC, technological innovations and synergies will accelerate, enabling powerful, flexible electronics previously only found in science fiction to become a reality.

Author contributions

TD, PC and SKM the idea, TD, PC and SKM written original manuscript. IL, JSG, RD and SKM read and edited the manuscript.

Conflicts of interest

The authors declare no conflicts of interest.

Acknowledgements

Satyendra K. Mishra thanks full to CTTC for providing infrastructure for this research. Rakesh Kumar Dubey thankful for the Insititute of Physics University of Szczecin polish national university for providing the fees for open access.

References

1 R. Crabb and F. Treble, *Nature*, 1967, **213**, 1223–1224.
2 T. Dutta, N. Yadav, Y. Wu, G. J. Cheng, X. Liang, S. Ramakrishna, A. Sbai, R. Gupta, A. Mondal, Z. Hongyu and A. Yadav, *Nano Mater. Sci.*, 2024, **6**, 1–23, DOI: 10.1016/j.nanoms.2023.05.003.
3 T. Dutta, T. Noushin, S. Tabassum and S. K. Mishra, *Sensors*, 2023, **23**, 6849.
4 J. Li, W. Guo, W. Zhao, Y. Zhu, J. Bai, Z. Xia, X. Zhou and Z. Liu, *eScience*, 2024, 100250, DOI: 10.1016/j.esci.2024.100250.
5 L. Hu, P. L. Chee, S. Sugiarto, Y. Yu, C. Shi, R. Yan, Z. Yao, X. Shi, J. Zhi and D. Kai, *Adv. Mater.*, 2023, **35**, 2205326.
6 Z. Liu, X. Luo, L. Qin, G. Fang and S. Liang, *Adv. Powder Mater.*, 2022, **1**, 100011.
7 L. Wang, D. Chen, K. Jiang and G. Shen, *Chem. Soc. Rev.*, 2017, **46**, 6764–6815.
8 Y.-n. Wang, C.-f. Dong, D.-w. Zhang, P.-p. Ren, L. Li and X.-g. Li, *Int. J. Miner., Metall. Mater.*, 2015, **22**, 998–1004.
9 F. Lang, J. Pang and X.-H. Bu, *eScience*, 2024, 100231, DOI: 10.1016/j.esci.2024.100231.
10 T. R. Ray, J. Choi, A. J. Bandodkar, S. Krishnan, P. Gutruf, L. Tian, R. Ghaffari and J. A. Rogers, *Chem. Rev.*, 2019, **119**, 5461–5533.
11 H. Yuk, B. Lu and X. Zhao, *Chem. Soc. Rev.*, 2019, **48**, 1642–1667.
12 S. Huang, Y. Liu, Y. Zhao, Z. Ren and C. F. Guo, *Adv. Funct. Mater.*, 2019, **29**, 1805924.
13 I. D. Joshipura, M. Finn, S. T. M. Tan, M. D. Dickey and D. J. Lipomi, *MRS Bull.*, 2017, **42**, 960–967.
14 M. L. Hammock, A. Chortos, B. C. K. Tee, J. B. H. Tok and Z. Bao, *Adv. Mater.*, 2013, **25**, 5997–6038.
15 S. P. Lacour, S. Wagner, Z. Huang and Z. Suo, *Appl. Phys. Lett.*, 2003, **82**, 2404–2406.
16 D. H. Kim, J. Xiao, J. Song, Y. Huang and J. A. Rogers, *Adv. Mater.*, 2010, **22**, 2108–2124.
17 T. Sekitani, Y. Noguchi, K. Hata, T. Fukushima, T. Aida and T. Someya, *Science*, 2008, **321**, 1468–1472.
18 S. C. Mannsfeld, B. C. Tee, R. M. Stoltenberg, C. V. H. Chen, S. Barman, B. V. Muir, A. N. Sokolov, C. Reese and Z. Bao, *Nat. Mater.*, 2010, **9**, 859–864.
19 S. Choi, S. I. Han, D. Kim, T. Hyeon and D.-H. Kim, *Chem. Soc. Rev.*, 2019, **48**, 1566–1595.
20 W. Wang, R. Narain and H. Zeng, *Front. Chem.*, 2018, **6**, 497.
21 J. Tavakoli and Y. Tang, *Polymers*, 2017, **9**, 364.
22 X. Liu, J. Liu, S. Lin and X. Zhao, *Mater. Today*, 2020, **36**, 102–124.
23 X. Zhao, *Soft matter*, 2014, **10**, 672–687.
24 Z. Deng, R. Yu and B. Guo, *Mater. Chem. Front.*, 2021, **5**, 2092–2123.
25 Q. Rong, W. Lei and M. Liu, *Chem.–Eur. J.*, 2018, **24**, 16930–16943.
26 A. Koivikko, V. Lampinen, K. Yiannacou, V. Sharma and V. Sariola, *IEEE Sens. J.*, 2021, **22**, 11241–11247.
27 A. Nathan, A. Ahnood, M. T. Cole, S. Lee, Y. Suzuki, P. Hiralal, F. Bonaccorso, T. Hasan, L. Garcia-Gancedo and A. Dyadyusha, *Proc. IEEE*, 2012, **100**, 1486–1517.
28 R. Lin, M. Lei, S. Ding, Q. Cheng, Z. Ma, L. Wang, Z. Tang, B. Zhou and Y. Zhou, *Mater. Today Bio*, 2023, **23**, 100787.
29 S. Mudhulu, M. Channegowda, S. Balaji, A. Khosla and P. Sekhar, *IEEE Sens. J.*, 2023, **23**, 18963–18976.
30 J. Tang, Y. He, D. Xu, W. Zhang, Y. Hu, H. Song, Y. Zhang, Y. M. Chen, Y. Yang and K. Zhang, *npj Flexible Electron.*, 2023, **7**, 28.
31 S. N. Banitaba, S. Khademolqorani, V. V. Jadhav, E. Chamanehpour, Y. K. Mishra, E. Mostafavi and A. Kaushik, *Mater. Today Bio*, 2023, **5**, 100055.
32 Y. Tang, L. Zhen, J. Liu and J. Wu, *Anal. Chem.*, 2013, **85**, 2787–2794.
33 Z.-Q. Ran, N. Ma and F.-C. Tsai, *IEEE International Flexible Electronics Technology Conference (IFETC)*, 2022, pp. 1–2.
34 A. Abodurexiti and X. Maimaitiyiming, *IEEE Sens. J.*, 2022, **22**, 12588–12594.
35 K. K. Yeung, T. Huang, Y. Hua, K. Zhang, M. M. F. Yuen and Z. Gao, *IEEE Sens. J.*, 2021, **21**, 14522–14539.
36 Y. Xiang and D. Chen, *Eur. Polym. J.*, 2007, **43**, 4178–4187.
37 S. J. Devaki, R. K. Narayanan and S. Sarojam, *Mater. Lett.*, 2014, **116**, 135–138.
38 Q. Peng, J. Chen, T. Wang, X. Peng, J. Liu, X. Wang, J. Wang and H. Zeng, *InfoMat*, 2020, **2**, 843–865.
39 X. Jing, H.-Y. Mi, B. N. Napiwocki, X.-F. Peng and L.-S. Turng, *Carbon*, 2017, **125**, 557–570.
40 S. Ying, Z. Ma, Z. Zhou, R. Tao, K. Yan, M. Xin, Y. Li, L. Pan and Y. Shi, *IEEE Access*, 2020, **8**, 189646–189660.

41 P. M. Gotovtsev, G. U. Badranova, Y. V. Zubavichus, N. K. Chumakov, C. G. Antipova, R. A. Kamyshinsky, M. Y. Presniakov, K. V. Tokaev and T. E. Grigoriev, *Heliyon*, 2019, **5**, e02498.
42 L. Li, Y. Wang, L. Pan, Y. Shi, W. Cheng, Y. Shi and G. Yu, *Nano letters*, 2015, **15**, 1146–1151.
43 Y. Guo, K. Zheng and P. Wan, *Small*, 2018, **14**, 1704497.
44 W. Li, J. Liu, J. Wei, Z. Yang, C. Ren and B. Li, *Adv. Funct. Mater.*, 2023, 2213485.
45 K. Wang, X. Zhang, C. Li, X. Sun, Q. Meng, Y. Ma and Z. Wei, *Adv. Mater.*, 2015, **27**, 7451–7457.
46 Y. Wang, Y. Shi, L. Pan, Y. Ding, Y. Zhao, Y. Li, Y. Shi and G. Yu, *Nano Lett.*, 2015, **15**, 7736–7741.
47 C. Arndt, M. Hauck, I. Wacker, B. Zeller-Plumhoff, F. Rasch, M. Taale, A. S. Nia, X. Feng, R. Adelung and R. R. Schröder, *Nano Lett.*, 2021, **21**, 3690–3697.
48 E. Fantino, A. Chiappone, I. Roppolo, D. Manfredi, R. Bongiovanni, C. F. Pirri and F. Calignano, *Adv. Mater.*, 2016, **28**, 3712–3717.
49 D. C. Hyun, M. Park, C. Park, B. Kim, Y. Xia, J. H. Hur, J. M. Kim, J. J. Park and U. Jeong, *Adv. Mater.*, 2011, **26**, 2946–2950.
50 V. Pardo-Yissar, R. Gabai, A. N. Shipway, T. Bourenko and I. Willner, *Adv. Mater.*, 2001, **13**, 1320–1323.
51 L. Janovák and I. Dékány, *Appl. Surf. Sci.*, 2010, **256**, 2809–2817.
52 P. Baei, S. Jalili-Firoozinezhad, S. Rajabi-Zeleti, M. Tafazzoli-Shadpour, H. Baharvand and N. Aghdami, *Mater. Sci. Eng., C*, 2016, **63**, 131–141.
53 Q.-B. Wei, Y.-L. Luo, C.-H. Zhang, L.-H. Fan and Y.-S. Chen, *Sens. Actuators, B*, 2008, **134**, 49–56.
54 L. Han, K. Liu, M. Wang, K. Wang, L. Fang, H. Chen, J. Zhou and X. Lu, *Adv. Funct. Mater.*, 2018, **28**, 1704195.
55 Y. Liang, X. Zhao, T. Hu, Y. Han and B. Guo, *J. Colloid Interface Sci.*, 2019, **556**, 514–528.
56 Z. Deng, T. Hu, Q. Lei, J. He, P. X. Ma and B. Guo, *ACS Appl. Mater. Interfaces*, 2019, **11**, 6796–6808.
57 L. Mottet, D. Le Cornec, J.-M. Noël, F. Kanoufi, B. Delord, P. Poulin, J. Bibette and N. Bremond, *Soft Matter*, 2018, **14**, 1434–1441.
58 Y. Liang, X. Zhao, T. Hu, B. Chen, Z. Yin, P. X. Ma and B. Guo, *Small*, 2019, **15**, 1900046.
59 Y. Wang, F. Huang, X. Chen, X.-W. Wang, W.-B. Zhang, J. Peng, J. Li and M. Zhai, *Chem. Mater.*, 2018, **30**, 4289–4297.
60 Y. Xu, Z. Lin, X. Huang, Y. Wang, Y. Huang and X. Duan, *Adv. Mater.*, 2013, **25**, 5779–5784.
61 X. Zhao, H. Wu, B. Guo, R. Dong, Y. Qiu and P. X. Ma, *Biomaterials*, 2017, **122**, 34–47.
62 J. Qu, X. Zhao, P. X. Ma and B. Guo, *Acta Biomater.*, 2018, **72**, 55–69.
63 B. Guo, J. Qu, X. Zhao and M. Zhang, *Acta Biomater.*, 2019, **84**, 180–193.
64 P. Chakraborty, T. Guterman, N. Adadi, M. Yadid, T. Brosh, L. Adler-Abramovich, T. Dvir and E. Gazit, *ACS Nano*, 2018, **13**, 163–175.
65 Z. Deng, Y. Guo, P. X. Ma and B. Guo, *J. Colloid Interface Sci.*, 2018, **526**, 281–294.
66 J. Chen, Q. Peng, T. Thundat and H. Zeng, *Chem. Mater.*, 2019, **31**, 4553–4563.
67 Z. Wang, H. Zhou, J. Lai, B. Yan, H. Liu, X. Jin, A. Ma, G. Zhang, W. Zhao and W. Chen, *J. Mater. Chem. C*, 2018, **6**, 9200–9207.
68 J. Hur, K. Im, S. W. Kim, J. Kim, D.-Y. Chung, T.-H. Kim, K. H. Jo, J. H. Hahn, Z. Bao and S. Hwang, *ACS Nano*, 2014, **8**, 10066–10076.
69 L. Han, L. Yan, M. Wang, K. Wang, L. Fang, J. Zhou, J. Fang, F. Ren and X. Lu, *Chem. Mater.*, 2018, **30**, 5561–5572.
70 D. Gan, L. Han, M. Wang, W. Xing, T. Xu, H. Zhang, K. Wang, L. Fang and X. Lu, *ACS Appl. Mater. Interfaces*, 2018, **10**, 36218–36228.
71 B. Lu, H. Yuk, S. Lin, N. Jian, K. Qu, J. Xu and X. Zhao, *Nat. Commun.*, 2019, **10**, 1043.
72 S. Das, P. Chakraborty, S. Mondal, A. Shit and A. K. Nandi, *ACS Appl. Mater. Interfaces*, 2016, **8**, 28055–28067.
73 P. Li, Z. Jin, L. Peng, F. Zhao, D. Xiao, Y. Jin and G. Yu, *Adv. Mater.*, 2018, **30**, 1800124.
74 Y. Zhou, B. He, Z. Yan, Y. Shang, Q. Wang and Z. Wang, *Sensors*, 2018, **18**, 569.
75 C. H. Yang, S. Zhou, S. Shian, D. R. Clarke and Z. Suo, *Mater. Horiz.*, 2017, **4**, 1102–1109.
76 S. Li, B. N. Peele, C. M. Larson, H. Zhao and R. F. Shepherd, *Adv. Mater.*, 2016, **28**, 9770–9775.
77 C. Larson, B. Peele, S. Li, S. Robinson, M. Totaro, L. Beccai, B. Mazzolai and R. Shepherd, *Science*, 2016, **351**, 1071–1074.
78 Y. Huang, M. Zhong, F. Shi, X. Liu, Z. Tang, Y. Wang, Y. Huang, H. Hou, X. Xie and C. Zhi, *Angew. Chem., Int. Ed.*, 2017, **56**, 9141–9145.
79 T. Liu, M. Liu, S. Dou, J. Sun, Z. Cong, C. Jiang, C. Du, X. Pu, W. Hu and Z. L. Wang, *ACS Nano*, 2018, **12**, 2818–2826.
80 O. Y. Kweon, S. K. Samanta, Y. Won, J. H. Yoo and J. H. Oh, *ACS Appl. Mater. Interfaces*, 2019, **11**, 26134–26143.
81 S. Liu, R. Zheng, S. Chen, Y. Wu, H. Liu, P. Wang, Z. Deng and L. Liu, *J. Mater. Chem. C*, 2018, **6**, 4183–4190.
82 X. P. Morelle, W. R. Illeperuma, K. Tian, R. Bai, Z. Suo and J. J. Vlassak, *Adv. Mater.*, 2018, **30**, 1801541.
83 Y. Si, L. Wang, X. Wang, N. Tang, J. Yu and B. Ding, *Adv. Mater.*, 2017, **29**, 1700339.
84 V. T. Tran, M. T. I. Mredha, S. K. Pathak, H. Yoon, J. Cui and I. Jeon, *ACS Appl. Mater. Interfaces*, 2019, **11**, 24598–24608.
85 Y. Deng, I. Hussain, M. Kang, K. Li, F. Yao, S. Liu and G. Fu, *Chem. Eng. J.*, 2018, **353**, 900–910.
86 J. Lai, H. Zhou, M. Wang, Y. Chen, Z. Jin, S. Li, J. Yang, X. Jin, H. Liu and W. Zhao, *J. Mater. Chem. C*, 2018, **6**, 13316–13324.
87 J. Wu, Z. Wu, S. Han, B.-R. Yang, X. Gui, K. Tao, C. Liu, J. Miao and L. K. Norford, *ACS Appl. Mater. Interfaces*, 2019, **11**, 2364–2373.
88 T. B. H. Schroeder, A. Guha, A. Lamoureux, G. VanRenterghem, D. Sept, M. Shtein, J. Yang and M. Mayer, *Nature*, 2017, **552**, 214–218.

89 X. Jing, H.-Y. Mi, Y.-J. Lin, E. Enriquez, X.-F. Peng and L.-S. Turng, *ACS Appl. Mater. Interfaces*, 2018, **10**, 20897–20909.
90 X. He, C. Zhang, M. Wang, Y. Zhang, L. Liu and W. Yang, *ACS Appl. Mater. Interfaces*, 2017, **9**, 11134–11143.
91 S. Liang, Y. Zhang, H. Wang, Z. Xu, J. Chen, R. Bao, B. Tan, Y. Cui, G. Fan and W. Wang, *Adv. Mater.*, 2018, **30**, 1704235.
92 X. Jing, H.-Y. Mi, X.-F. Peng and L.-S. Turng, *Carbon*, 2018, **136**, 63–72.
93 C. Tondera, T. F. Akbar, A. K. Thomas, W. Lin, C. Werner, V. Busskamp, Y. Zhang and I. R. Minev, *Small*, 2019, **15**, 1901406.
94 M. Hua, S. Wu, Y. Ma, Y. Zhao, Z. Chen, I. Frenkel, J. Strzalka, H. Zhou, X. Zhu and X. He, *Nature*, 2021, **590**, 594–599.
95 J. W. Goodwin and R. W. Hughes, *Rheology for Chemists: an Introduction*, Royal Society of Chemistry, 2008.
96 E. Y. Kang, H. J. Moon, M. K. Joo and B. Jeong, *Biomacromolecules*, 2012, **13**, 1750–1757.
97 Y. Wang, Y. Yu, J. Guo, Z. Zhang, X. Zhang and Y. Zhao, *Adv. Funct. Mater.*, 2020, **30**, 2000151.
98 W. Cui, M.-H. Pi, Y.-S. Li, L.-Y. Shi and R. Ran, *ACS Appl. Polym. Mater.*, 2020, **2**, 3378–3389.
99 H. Kim and W.-J. Maeng, *Thin Solid Films*, 2009, **517**, 2563–2580.
100 Y. Gong, D. Palacio, X. Song, R. L. Patel, X. Liang, X. Zhao, J. B. Goodenough and K. Huang, *Nano Lett.*, 2013, **13**, 4340–4345.
101 C. L. Everhart, K. E. Kaplan, M. M. Winterkorn, H. Kwon, J. Provine, M. Asheghi, K. E. Goodson, F. B. Prinz and T. W. Kenny, *IEEE Micro Electro Mechanical Systems (MEMS)*, 2018, pp. 976–979.
102 D. Metzler, C. Li, S. Engelmann, R. L. Bruce, E. A. Joseph and G. S. Oehrlein, *J. Vac. Sci. Technol., A*, 2016, **34**(1), 01B101.
103 S. D. Sherpa and A. Ranjan, *J. Vac. Sci. Technol., A*, 2017, **35**(1), 01A102.
104 K. S. Kim, K. H. Kim, Y. Nam, J. Jeon, S. Yim, E. Singh, J. Y. Lee, S. J. Lee, Y. S. Jung and G. Y. Yeom, *ACS Appl. Mater. Interfaces*, 2017, **9**, 11967–11976.
105 X. Li, M. Bao and S. Shen, *Sens. Actuators, A*, 1996, **57**, 47–52.
106 M. Mansoor, I. Haneef, A. De Luca, J. Coull and F. Udrea, *J. Micromech. Microeng.*, 2018, **28**, 085013.
107 X. Liu, M. Mwangi, X. Li, M. O'Brien and G. M. Whitesides, *Lab Chip*, 2011, **11**, 2189–2196.
108 J. Bas, T. Dutta, I. Llamas Garro, J. S. Velázquez-González, R. Dubey and S. K. Mishra, *Sensors*, 2024, **24**, 1955.
109 C.-C. Kim, H.-H. Lee, K. H. Oh and J.-Y. Sun, *Science*, 2016, **353**, 682–687.
110 G. Gao, F. Yang, F. Zhou, J. He, W. Lu, P. Xiao, H. Yan, C. Pan, T. Chen and Z. L. Wang, *Adv. Mater.*, 2020, **32**, 2004290.
111 D. Buenger, F. Topuz and J. Groll, *Prog. Polym. Sci.*, 2012, **37**, 1678–1719.
112 L. Wang, T. Xu and X. Zhang, *TrAC, Trends Anal. Chem.*, 2021, **134**, 116130.
113 Y. Gao, S. Gu, F. Jia and G. Gao, *J. Mater. Chem. A*, 2020, **8**, 24175–24183.
114 Z. Lei and P. Wu, *Nat. Commun.*, 2019, **10**, 3429.
115 L. Dong, A. K. Agarwal, D. J. Beebe and H. Jiang, *Nature*, 2006, **442**, 551–554.
116 X.-H. Li, C. Liu, S.-P. Feng and N. X. Fang, *Joule*, 2019, **3**, 290–302.
117 W. Yu, O. Deschaume, L. Dedroog, C. J. Garcia Abrego, P. Zhang, J. Wellens, Y. de Coene, S. Jooken, K. Clays, W. Thielemans, C. Glorieux and C. Bartic, *Adv. Funct. Mater.*, 2022, **32**, 2108234.
118 A. Tamayol, M. Akbari, Y. Zilberman, M. Comotto, E. Lesha, L. Serex, S. Bagherifard, Y. Chen, G. Fu and S. K. Ameri, *Adv. Healthcare Mater.*, 2016, **5**, 624.
119 Z. Xu, J. Song, B. Liu, S. Lv, F. Gao, X. Luo and P. Wang, *Sens. Actuators, B*, 2021, **348**, 130674.
120 K. H. Lee, Y. Z. Zhang, H. Kim, Y. Lei, S. Hong, S. Wustoni, A. Hama, S. Inal and H. N. Alshareef, *Small Methods*, 2021, **5**, 2100819.
121 J. Wu, K. Tao, Y. Guo, Z. Li, X. Wang, Z. Luo, S. Feng, C. Du, D. Chen, J. Miao and L. K. Norford, *Adv. Sci.*, 2017, **4**, 1600319.
122 J. Wu, Z. Wu, H. Ding, Y. Wei, W. Huang, X. Yang, Z. Li, L. Qiu and X. Wang, *ACS Appl. Mater. Interfaces*, 2020, **12**, 2634–2643.
123 Z. Wu, L. Rong, J. Yang, Y. Wei, K. Tao, Y. Zhou, B.-R. Yang, X. Xie and J. Wu, *Small*, 2021, **17**, 2104997.
124 Z. Wu, H. Wang, Q. Ding, K. Tao, W. Shi, C. Liu, J. Chen and J. Wu, *Adv. Funct. Mater.*, 2023, **33**, 2300046.
125 L. Liu, T. Fei, X. Guan, X. Lin, H. Zhao and T. Zhang, *Sens. Actuators, B*, 2020, **320**, 128318.
126 L. Liu, T. Fei, X. Guan, H. Zhao and T. Zhang, *Biosens. Bioelectron.*, 2021, **191**, 113459.
127 R. Wang, M. Zhang, Y. Guan, M. Chen and Y. Zhang, *Soft Matter*, 2019, **15**, 6107–6115.
128 J. Wu, K. Tao, J. Zhang, Y. Guo, J. Miao and L. K. Norford, *J. Mater. Chem. A*, 2016, **4**, 8130–8140.
129 X. Sun, Y. Wang and Y. Lei, *Chem. Soc. Rev.*, 2015, **44**, 8019–8061.
130 G. Wang, Y. Li, Z. Cai and X. Dou, *Adv. Mater.*, 2020, **32**, 1907043.
131 Y. Luo, J. Li, Q. Ding, H. Wang, C. Liu and J. Wu, *Nano-Micro Lett.*, 2023, **15**, 136.
132 J. Y. Sun, C. Keplinger, G. M. Whitesides and Z. Suo, *Adv. Mater.*, 2014, **26**, 7608–7614.
133 F. Zhan, Z. Wang, T. Wu, Q. Dong, C. Zhao, G. Wang and J. Qiu, *J. Mater. Chem. A*, 2018, **6**, 4981–4987.
134 M. Alshawabkeh and L.-M. Faller, in *Smart Materials in Additive Manufacturing*, Elsevier, 2022, pp. 335–371.
135 Z. Deng, Y. Guo, X. Zhao, P. X. Ma and B. Guo, *Chem. Mater.*, 2018, **30**, 1729–1742.
136 C. Li, H. Zheng, X. Zhang, Z. Pu and D. Li, *Chem. Synth.*, 2024, **4**, 17.
137 S. Cai, B. Niu, X. Ma, S. Wan and X. He, *Chem. Eng. J.*, 2022, **430**, 132957.
138 S. Zheng, H. Wang, P. Das, Y. Zhang, Y. Cao, J. Ma, S. Liu and Z.-S. Wu, *Adv. Mater.*, 2021, **33**, 2005449.

139 T. Someya, Y. Kato, T. Sekitani, S. Iba, Y. Noguchi, Y. Murase, H. Kawaguchi and T. Sakurai, *Proc. Natl. Acad. Sci. U. S. A.*, 2005, **102**, 12321–12325.
140 Y. Wang, R. Yang, Z. Shi, L. Zhang, D. Shi, E. Wang and G. Zhang, *ACS Nano*, 2011, **5**, 3645–3650.
141 D. J. Lipomi, M. Vosgueritchian, B. C. Tee, S. L. Hellstrom, J. A. Lee, C. H. Fox and Z. Bao, *Nat. Nanotechnol.*, 2011, **6**, 788–792.
142 J. Duan, X. Liang, J. Guo, K. Zhu and L. Zhang, *Adv. Mater.*, 2016, **28**, 8037–8044.
143 Z. Lei, Q. Wang, S. Sun, W. Zhu and P. Wu, *Adv. Mater.*, 2017, **29**, 1700321.
144 M. Liao, P. Wan, J. Wen, M. Gong, X. Wu, Y. Wang, R. Shi and L. Zhang, *Adv. Funct. Mater.*, 2017, **27**, 1703852.
145 J. Zhang, H. Yao, J. Mo, S. Chen, Y. Xie, S. Ma, R. Chen, T. Luo, W. Ling, L. Qin, Z. Wang and W. Zhou, *Nat. Commun.*, 2022, **13**, 5076.
146 N. Elboughdiri, S. Iqbal, S. Abdullaev, M. Aljohani, A. Safeen, K. Althubeiti and R. Khan, *RSC Adv.*, 2023, **13**, 35993–36008.
147 S. Chun, J.-S. Kim, Y. Yoo, Y. Choi, S. J. Jung, D. Jang, G. Lee, K.-I. Song, K. S. Nam and I. Youn, *Nat. Electron.*, 2021, **4**, 429–438.
148 Y. Luo, M. R. Abidian, J.-H. Ahn, D. Akinwande, A. M. Andrews, M. Antonietti, Z. Bao, M. Berggren, C. A. Berkey and C. J. Bettinger, *ACS Nano*, 2023, **17**, 5211–5295.
149 V. R. Feig, H. Tran, M. Lee and Z. Bao, *Nat. Commun.*, 2018, **9**, 2740.
150 T. Zhu, Y. Ni, G. M. Biesold, Y. Cheng, M. Ge, H. Li, J. Huang, Z. Lin and Y. Lai, *Chem. Soc. Rev.*, 2023, **52**, 473–509.
151 H. Peng, Y. Xin, J. Xu, H. Liu and J. Zhang, *Mater. Horiz.*, 2019, **6**, 618–625.
152 H. Liao, X. Guo, P. Wan and G. Yu, *Adv. Funct. Mater.*, 2019, **29**, 1904507.
153 Y.-Z. Zhang, K. H. Lee, D. H. Anjum, R. Sougrat, Q. Jiang, H. Kim and H. N. Alshareef, *Sci. Adv.*, 2018, **4**, eaat0098.
154 F. Fu, J. Wang, H. Zeng and J. Yu, *ACS Mater. Lett.*, 2020, **2**, 1287–1301.
155 Y. Yang, Y. Yang, Y. Cao, X. Wang, Y. Chen, H. Liu, Y. Gao, J. Wang, C. Liu and W. Wang, *Chem. Eng. J.*, 2021, **403**, 126431.
156 Y. Wu, Y. Luo, T. J. Cuthbert, A. V. Shokurov, P. K. Chu, S. P. Feng and C. Menon, *Adv. Sci.*, 2022, **9**, 2106008.
157 Y. Hu, M. Zhang, C. Qin, X. Qian, L. Zhang, J. Zhou and A. Lu, *Carbohydr. Polym.*, 2021, **265**, 118078.
158 W. Xu, L. B. Huang, M. C. Wong, L. Chen, G. Bai and J. Hao, *Adv. Energy Mater.*, 2017, **7**, 1601529.
159 X. Lu, L. Zheng, H. Zhang, W. Wang, Z. L. Wang and C. Sun, *Nano Energy*, 2020, **78**, 105359.
160 Z. Zhao, Y.-P. Hu, K.-Y. Liu, W. Yu, G.-X. Li, C.-Z. Meng and S.-J. Guo, *Gels*, 2023, **9**, 257.
161 X. Qian and A. Lu, *ACS Appl. Polym. Mater.*, 2021, **3**, 3747–3754.
162 F. Sheng, J. Yi, S. Shen, R. Cheng, C. Ning, L. Ma, X. Peng, W. Deng, K. Dong and Z. L. Wang, *ACS Appl. Mater. Interfaces*, 2021, **13**, 44868–44877.
163 K. Zhang, L. Cai and G. Chen, *Polymer*, 2019, **167**, 154–158.
164 S. Chun, A. Hong, Y. Choi, C. Ha and W. Park, *Nanoscale*, 2016, **8**, 9185–9192.
165 R. Khan, N. U. Rehman, S. Iqbal, S. Abdullaev and H. M. Aldosari, *ACS Appl. Electron. Mater.*, 2024, **6**, 73–119.
166 R. Khan, N. U. Rehman, N. Ilyas, N. Sfina, M. Barhoumi, A. Khan, K. Althubeiti, S. A. Otaibi, S. Iqbal, N. Rahman, M. Sohail, A. Ullah, T. Del Rosso, Q. Zaman, A. Ali Khan, S. S. Abdullaev and A. Khan, *Nanoscale*, 2023, **15**, 1900–1913.
167 T. Shi, R. Wang, Z. Wu, Y. Sun, J. An and Q. Liu, *Small Struct.*, 2021, **2**, 2000109.
168 T.-C. Chang, K.-C. Chang, T.-M. Tsai, T.-J. Chu and S. M. Sze, *Mater. Today*, 2016, **19**, 254–264.
169 R. Khan, N. U. Rehman, N. Ilyas, N. Sfina, M. Barhoumi, A. Khan, K. Althubeiti, S. Al Otaibi, S. Iqbal and N. Rahman, *Nanoscale*, 2023, **15**, 1900–1913.
170 R. Khan, N. Ilyas, M. Z. M. Shamim, M. I. Khan, M. Sohail, N. Rahman, A. A. Khan, S. N. Khan and A. Khan, *J. Mater. Chem. C*, 2021, **9**, 15755–15788.
171 C.-C. Lin, P.-H. Chen, M.-C. Chen, T.-C. Chang, C.-Y. Lin, H.-X. Zheng, C.-K. Chen, W.-C. Huang, W.-C. Chen and H.-C. Huang, *IEEE Trans. Electron Devices*, 2019, **66**, 2595–2599.
172 M. Qi, C. Guo and M. Zeng, *J. Nanomater.*, 2019, 6724018.
173 J. T. Qiu, S. Samanta, M. Dutta, S. Ginnaram and S. Maikap, *Langmuir*, 2019, **35**, 3897–3906.
174 A. D. Kent and D. C. Worledge, *Nat. Nanotechnol.*, 2015, **10**, 187–191.
175 S. Raoux, W. Wełnic and D. Ielmini, *Chem. Rev.*, 2010, **110**, 240–267.
176 R. Waser and M. Aono, *Nat. Mater.*, 2007, **6**, 833–840.
177 P. Y. Lai and J.-S. Chen, *IEEE Electron Device Lett.*, 2011, **32**, 387–389.
178 S. Seo, M. Lee, D. Seo, E. Jeoung, D.-S. Suh, Y. Joung, I. Yoo, I. Hwang, S. Kim and I. Byun, *Appl. Phys. Lett.*, 2004, **85**, 5655–5657.
179 F. Zhao, J. Bae, X. Zhou, Y. Guo and G. Yu, *Adv. Mater.*, 2018, **30**, 1801796.
180 Y. Huang, Z. Li, Z. Pei, Z. Liu, H. Li, M. Zhu, J. Fan, Q. Dai, M. Zhang and L. Dai, *Adv. Energy Mater.*, 2018, **8**, 1802288.
181 C. Qin and A. Lu, *Carbohydr. Polym.*, 2021, **274**, 118667.
182 H. Chen, J. Huang, J. Liu, J. Gu, J. Zhu, B. Huang, J. Bai, J. Guo, X. Yang and L. Guan, *J. Mater. Chem. A*, 2021, **9**, 23243–23255.
183 Q. Zhang, Y. Jiang, L. Chen, W. Chen, J. Li, Y. Cai, C. Ma, W. Xu, Y. Lu and X. Jia, *Adv. Funct. Mater.*, 2021, **31**, 2100686.
184 A. Shastri, L. M. McGregor, Y. Liu, V. Harris, H. Nan, M. Mujica, Y. Vasquez, A. Bhattacharya, Y. Ma and M. Aizenberg, *Nat. Chem.*, 2015, **7**, 447–454.
185 M.-J. Yin, Z. Yin, Y. Zhang, Q. Zheng and A. P. Zhang, *Nano Energy*, 2019, **58**, 96–104.

186 Z. Shen, X. Zhu, C. Majidi and G. Gu, *Adv. Mater.*, 2021, **33**, 2102069.
187 X. Pei, H. Zhang, Y. Zhou, L. Zhou and J. Fu, *Mater. Horiz.*, 2020, **7**, 1872–1882.
188 J. H. Kwon, Y. M. Kim and H. C. Moon, *ACS Nano*, 2021, **15**, 15132–15141.
189 X. Bai, Y. Yu, H. H. Kung, B. Wang and J. Jiang, *J. Power Sources*, 2016, **306**, 42–48.